Solar Energy 198 (2020) 247–274

Contents lists available at ScienceDirect

Solar Energy

journal homepage: www.elsevier.com/locate/solener

Review on novel single-phase grid-connected solar inverters: Circuits and control methods

Ersan Kabalcı

Department of Electrical and Electronics Engineering, Faculty of Engineering and Architecture, Nevsehir Haci Bektas Veli University, 50300 Nevsehir, Turkey

ARTICLE INFO

Keywords:
Grid-connected inverter
Micro inverter
Solar inverter
PLL
MPPT
Evolutionary MPPT

ABSTRACT

An ever-increasing interest on integrating solar power to utility grid exists due to wide use of renewable energy sources and distributed generation. The grid-connected solar inverters that are the key devices interfacing solar power plant with utility play crucial role in this situation. Although three-phase inverters were industry standard in large photovoltaic (PV) power plant applications, the microgrid regulations increased the use of single-phase inverters in residential power plants and grid interconnection. This paper presents a detailed review on single-phase grid-connected solar inverters in terms of their improvements in circuit topologies and control methods. Even though there are many reviews have been proposed in the current literature, this study provides a differentiating approach by focusing on novel circuit topologies and control methods of string and micro inverters. The single and multi-stage solar inverters are reviewed in terms of emerging DC-DC converter and unfolding inverter topologies while the novel control methods of both stages have been surveyed in a comprehensive manner. The isolated and transformerless circuit topologies have been investigated by reviewing experimental and commercial devices. The soft computing, evolutionary and swarm intelligence based algorithms have been summarized in MPPT methods section while current injection and grid-connection control methods of unfolding inverters stage have been presented with and without PLL architecture. There are many papers have been compared and listed in each section to provide further outcomes which is followed by a summarizing discussion section and conclusion.

1. Introduction

The use of renewable energy sources (RESs) is increasing day by day in electricity generation due to their variety and support to utility grids. Besides the opportunities, the wide integrations of RESs to utility grid have brought several challenges in terms of planning, operating, maintenance and management issues. The distributed generation (DG) policies set by governments and demand side management (DSM) requirements of distribution system operators (DSOs) have leveraged the interoperability plans for generation plants including solar photovoltaics (PVs), wind turbines, fuel cells, and micro sources. A DG system comprised by various type of energy sources requires appropriate power electronic devices for power conversion for coupling at a single bus bar. The grid-connected inverters which are required for RES and DG integration to utility play crucial role in resource management. Moreover, the DC-DC converters are also required for regulating the DC power generated by PV or fuel cell sources while inverters are interfacing the entire power plant with grid (Kabalci, 2015; Kabalci and Kabalci, 2018, 2017).

The microgrid applications have promoted efficient power conversion requirements especially in low-voltage range (Schweizer and Kolar, 2013) where the wide variety of power converter studies on DC-DC converters and cascaded multilevel inverters have been proposed in the literature. The PV power plants hold the biggest share by increasing their installed capacity up to 400 GWp by the end of 2017 which is estimated to tackle 1000 GWp capacity by 2022 (Jaeger-Waldau, 2017; Masson et al., 2018; Schmela, 2018). The total installed capacity of global PV power plants has been increased more than 100 GWp in 2017 as seen in Fig. 1. The main contribution is supported by subsidies provided by US and European governments. The decreased installation and generation costs of PV technology promise that increment of PV power plants will tackle other RESs. Although the installed capacity of PV power plants is increasing, the overall efficiency which depends on efficiencies of PV module, power converters and control methods pursue their importance. The main sections of a power converter which is comprised by DC-DC converters, inverter stages and control methods are reviewed in several studies (Çelik et al., 2018; Meneses et al., 2013; Romero-Cadaval et al., 2013). The commercial and industrial PV inverter topologies have been improved to obtain maximum efficiency, low cost, lower sizes in terms of weights and

E-mail address: kabalci@nevsehir.edu.tr.

https://doi.org/10.1016/j.solener.2020.01.063
Received 16 October 2019; Received in revised form 16 January 2020; Accepted 22 January 2020

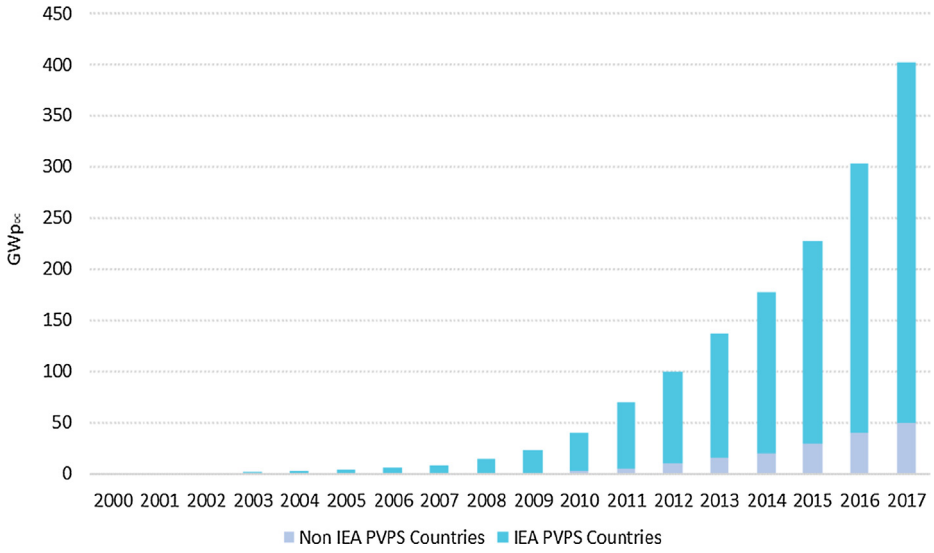

Fig. 1. Increment of installed global PV capacity (Masson et al., 2018).

volumes comparing to isolated inverters. Furthermore, the solar array strings and configurations are effective on obtaining maximum efficiency under partial shading conditions (Shams El-Dein et al., 2013a, 2013b).

The main target of a PV power converter is to harvest available maximum power from PV beam and transferring to utility grid. Thus, the control algorithms known as maximum power point tracking (MPPT) play crucial role on maximizing the yielded output power from a PV array. The whole configuration defined by PV arrays determine the arrangement of power converter and control methods. Although there are several definitions exist on power converter types used in grid connection of PV power plants, three main categories are the most common topologies as centralized, string and multi-string inverter (Díez-Mediavilla et al., 2014; Romero-Cadaval et al., 2013; Shayestegan et al., 2018; Sridhar and Umashankar, 2017; Zeb et al., 2018).

There have been numerous studies presenting single-phase and three-phase inverter topologies in the literature. The most common PV inverter configurations are illustrated in Fig. 2 where the centralized PV inverters are mainly used at high power solar plants with the PV modules connected in series and parallel configurations to yield combined output. The conventional centralized inverters have been used for long years in PV plants due to their power density and MW scale conversion capabilities. The main configuration of central inverters is designed to interface large PV power plants to the utility grid. The central inverter topologies are mostly based on two-level (2L) full bridges or recent three-level (3L) configurations such as neutral point clamped (NPC), conventional H-bridge (H4), T-type or emerging voltage source inverter (VSI) topologies.

The main idea behind using these inverter topologies is their single DC bus requirement which can be easily met by a simple DC-coupling of PV power plants. The DC bus voltage is mostly kept lower than 1000 V limit of PV module insulation range and typically up to 800 V to prevent overvoltage risks of large PV array strings. The output stage of an inverter is comprised by a line frequency (LF) three-phase transformer that decreases losses and increases the low voltage (LV) output for providing a connection to medium voltage (MV) distribution lines. The widespread topologies of central inverters provide efficiency around 85–90% and they are produced in bulky and heavy structures due to transformers and coolers. Besides, the 2L inverter topologies cause higher total harmonic distortion (THD) ratio and lower power factor comparing to 3L topologies (Jana et al., 2017; Kouro et al., 2015).

While the first central inverters were based on thyristors as switching devices, they have been evolved to power converters using MOSFET and insulated gate bipolar transistor (IGBT). The increased switching frequency have tackled some of aforementioned deficiencies such as poor power quality and higher THD, but they are still far from ensuring the desired overall efficiency (Ankit et al., 2018; Goroohi Sardou et al., 2018; Jana et al., 2017).

The most recent centralized inverter configurations are comprised by using 3L-NPC or 3L T-type inverter topologies which are shown in Fig. 3a and b respectively (Kouro et al., 2015). The 3L-NPC provides constant common mode voltage (CMV) and low THD ratio comparing to conventional inverter topologies. However, it requires higher isolation and high number of switching devices for inverter configuration. The rated power of a single central inverter is mostly lower than 1 MW to increase power efficiency. The constant CMV that is supplied by neutral point of 3L-NPC DC bus increases its advantages against conventional H4 inverter topology. Therefore, the transformerless operation does not cause any leakage current problem or modulation deficiencies in 3L-NPC topology. The T-type topology which is introduced by Conergy is used to clamp the phase voltage of utility grid to comprise a zero-voltage level by using two-way switching semiconductors. Thus, 3L T-type inverter can operate without any transformer at the output as 3L-NPC topology does (Ahmad and Singh, 2018; Faraji et al., 2017; Kouro et al., 2015).

The main drawback of centralized type inverter is the use of single MPPT algorithm which limits the overall efficiency regarding to the mostly shaded solar array. The string inverter is an undersized type of centralized inverter since each string is directly connected to an inverter and, total power capacity is increased with coupled inverter arrays. In string inverter configuration, an additional boost transformer or DC-DC boost converter is required if the string voltage is not high enough. The multi string PV inverters based on boost DC-DC converters with lower cost and lower size are improved to tackle this drawbacks since they associate the advantages of centralized and string inverters due to their flexible design features (Kabalci et al., 2015c, 2015b, 2015a; Romero-Cadaval et al., 2013).

The string inverters are essential to integrate any PV string with dedicated MPPT control to utility grid. The configuration of this inverter type is mostly implemented in single-stage or two-stage topologies regarding to including a DC-DC stage before inverter section or being comprised by just a single inverter stage. The two-stage inverters are equipped with MPPT control at DC-DC conversion stage, and supplies regulated DC bus voltage to input terminals of inverter.

On the other hand, unfolding inverter stage can be implemented with or without galvanic isolation depending on the use of line

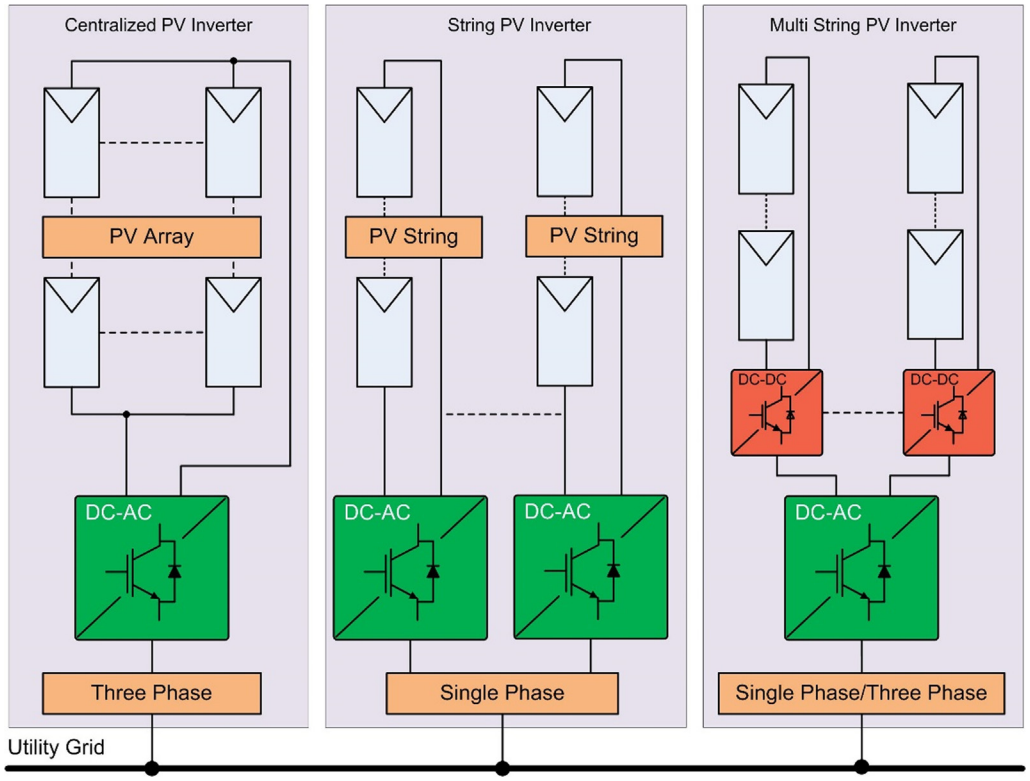

Fig. 2. PV inverter configurations.

transformer at the output stage. Besides heavy and bulky LF transformers, it is possible to use high frequency (HF) transformer to enable galvanic isolation at the converter stage. Any architecture including isolated or non-isolated topologies with single or two-stage has led to implementation of different string inverter topologies as shown in Fig. 4. The transformerless inverter topologies are preferred due to their reduced cost and higher efficiency opportunities comparing to isolated devices. On the other hand, the isolation requirements are met by using capacitive isolation providing to overcome voltage fluctuations and grounding issues in transformerless topologies.

The most common inverter topologies used in string PV inverters are conventional H4 topology, improved H5 topology, highly efficient and reliable inverter concept (HERIC), and H6 configurations. The recent achievements in circuit topologies and control methods have leveraged the overall efficiency of string inverters up to 97%-98% according to producer data provided by SMA, Danfoss, Delta and others (Gotekar et al., 2015; Guo et al., 2016; Zeb et al., 2018). Fig. 4 illustrates a collection of the most widely used circuit topologies of industrial and residential string inverters. The conventional H-bridge topology which is named as H4 is an industry standard in string inverters, but the modified and improved varieties of H4 are also used to increase efficiency and power quality of inverter. The common objective of H4, H6, NPC and T-type topologies is to stabilize the CMV in operation. The second inverter category comprised by H5 and HERIC topologies are improved to prevent circulating leakage currents owing to additional switching semiconductors (Rizzoli et al., 2016).

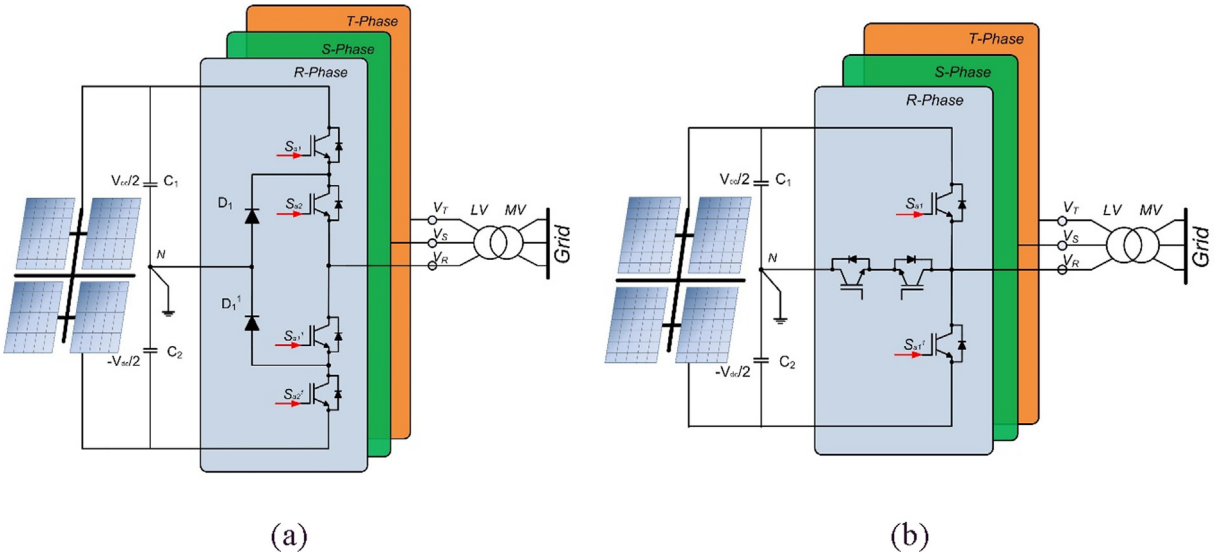

Fig. 3. Centralized PV inverter configurations, (a) 3L-NPC topology, (b) 3L T-type topology.

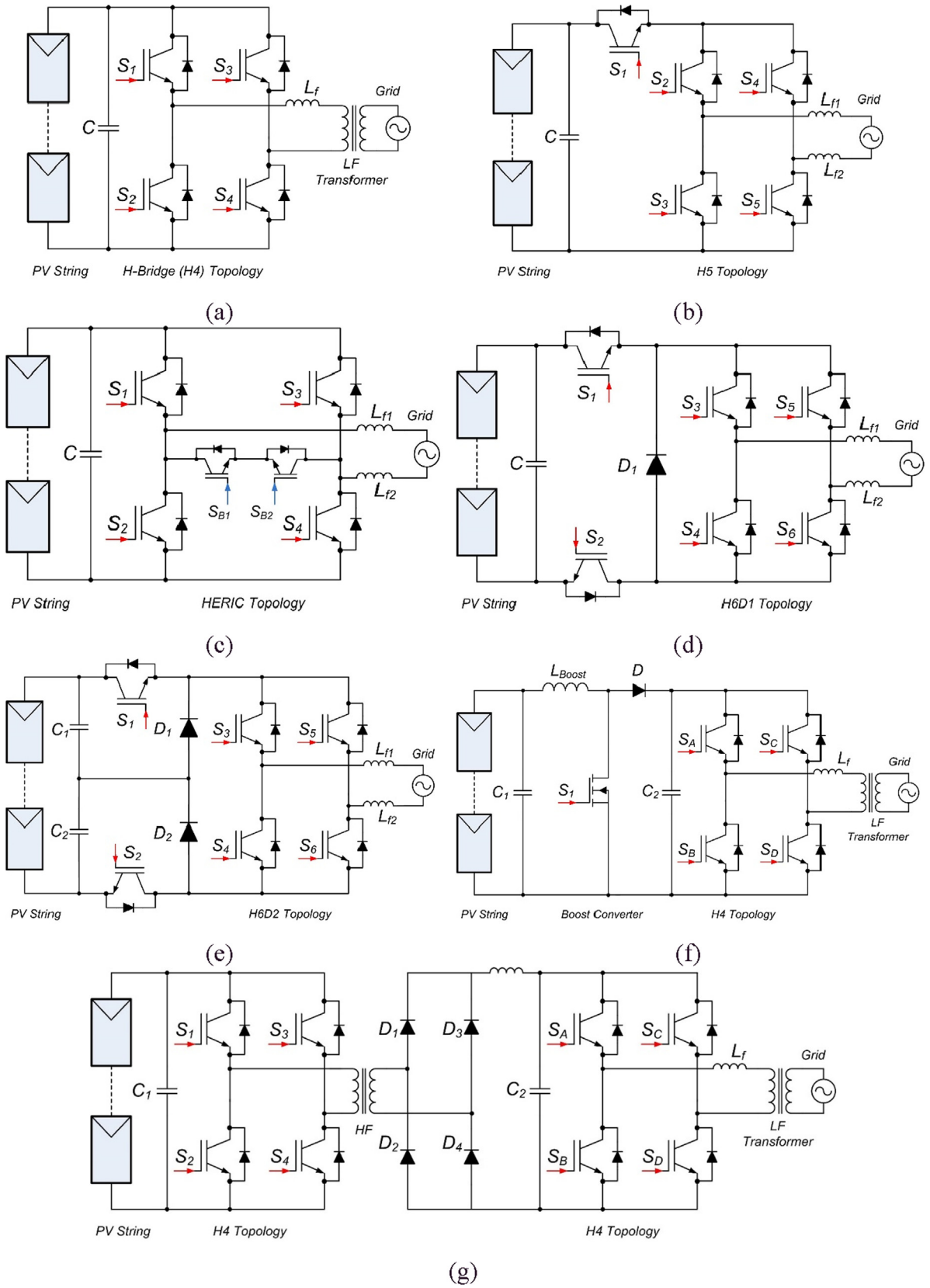

Fig. 4. String PV inverter topologies, (a) H4 topology, (b) H5 topology, (c) HERIC topology, (d) H6D1 topology, (e) H6D2 topology, (f) two-stage topology, (g) isolated two-stage dual active bridge topology.

Table 1
Comparison of H5, H6, and HERIC topologies.

Switching Frequency (kHz)	H5 (W)	H6 (W)	HERIC (W)
10	79.64	79.30	66.60
15	91.43	88.10	78.10
20	103.22	98.89	89.89
25	115.02	108.35	101.68

Three fundamental modulation schemes used for controlling the H4 and H5 topologies seen in Fig. 4a and b are unipolar, bipolar and hybrid methods. It is noted that the unipolar and hybrid modulation methods generate three-level output voltages with lower core losses but higher leakage current in isolated device configuration. On the other hand, the bipolar modulator causes two-level output voltage with higher core losses and lower leakage current. Therefore, it is suggested to use bipolar sinusoidal pulse width modulation (SPWM) method to decrease the leakage current magnitudes and filter requirement (Ahmad and Singh, 2017a, 2017b; Islam and Mekhilef, 2014; Rizzoli et al., 2016). The HERIC topology which is implemented to eliminate CM leakage current improves the overall efficiency comparing to H4 topology due to its AC bypass networks as shown in Fig. 4c. The bypass switching generates zero-level voltage output and interrupts the reactive power flow between filter and DC bus capacitor (Islam et al., 2015; Kouro et al., 2015; Zeb et al., 2018). Xiao et al. (2011) have noted that the HERIC topology has the least switching loss comparing to H5 and H6 topologies. However, HERIC itself represents the worst characteristics in terms of CM while H6 is noted as the best one among others. Xiao et al. have implemented a generic testbed to compare efficiency and operation conditions of three topologies where the input voltage varies between 340 and 700 V_{dc}, and rated power at 1000 W. The filter inductances have been defined as 4 mH while a 6.6 μF capacitor has been used as filter capacitance. The common mode capacitors are used as 2.2 nF for each device topology where the switching loss analysis results under various switching frequencies are shown in Table 1 (Xiao et al., 2011).

The H6 topology which is introduced by Ingeteam is an improved structure with an additional switch on negative DC bus of H5 topology. It has been developed in two different configurations as seen in Fig. 4d and e that are named H6D1 and H6D2 respectively implying the number of capacitive dividers and diode arrangements. Both configurations prevent interaction of freewheeling diodes with passive components and thus, they enable to obtain unipolar output comparing to H5 topology. Moreover, the leakage currents are eliminated due to freewheeling diodes (Islam et al., 2015; Kouro et al., 2015). The surveyed researches have shown that the transformerless inverter topologies are the most advantageous among others owing to several ways known in the literature to minimize the leakage current without decreasing the efficiency and eliminating the transformer requirements (Dutta et al., 2018; Kerekes et al., 2011; Meneses et al., 2013; Romero-Cadaval et al., 2013; Serban et al., 2017).

It can be noted that the most recent tendency for solar inverters is transformerless, single-stage and single-phase configurations as they have been surveyed in several papers (Dutta et al., 2018; Kerekes et al., 2011; Meneses et al., 2013; Romero-Cadaval et al., 2013). The galvanic isolation is built on the DC-DC side at the output of converter or on the AC side at the output of inverter with bulky line transformer. Although any of these configurations are preferred for safety, the efficiency of the entire device is drastically limited due to required components. On the other hand, the transformerless inverters are widely accepted in commercial and industrial applications owing to their higher efficiency, smaller size, and lower weight and volumes. The efficiency, weight, and volume of more than 400 different commercially available inverters have been compared in Kerekes et al. (2011) where results denote that transformerless topologies increase the overall efficiency up to 3% comparing to other topologies using HF or LF transformers. In addition to efficiency, the weight, cost, and size of transformerless topologies are obviously lower than others. The mid-point dc link capacitor and PV capacitors provide successful solutions for replacing galvanic isolation in terms of eliminating leakage current and parasitic capacitance (Kerekes et al., 2011). The two-stage inverter topologies presented in Fig. 4f and g are used as transformerless topologies as well as shown in their illustrated configurations. The conventional boost topology, flyback and interleaved converter topologies are widely used in two-stage configurations. On the other hand, dual active bridge (DAB) topologies seen in Fig. 4g are widely conducted in string and multi-string PV inverters due to their three-level output voltage generation capability. Although the string inverters improve MPPT efficiency replacing the single MPPT deficiency of central inverters, it suffers efficiency loss when any of PV module is shaded in a string. The shading and energy loss issues forced to shift solar inverter technologies from string inverter to micro inverters that are located at each module in a PV string or array.

Thus, the shading problem is limited to effect just only the shaded module instead of entire string. The micro inverters have been developed and widely used in low-power residential PV systems (Meneses et al., 2013). The micro inverter configurations are improved to provide MPPT control for each PV module and the rated power is generally between 100 and 400 W for any inverter to handle maximum power rate of a single PV module. The emerging micro inverter technology is based on mimicking the device topologies presented in Fig. 4. The micro inverters are also categorized according to isolation and inverter stage number as presented in string inverters. The recent two-stage micro inverters are implemented with HF transformers in order to decrease size and volume while non-isolated inverter are seen in single-stage or multi-stage configurations such as two-stage or three-stage topologies (Çelik et al., 2018; Khan et al., 2017; Petreuş et al., 2013; Rajgor, 2013; Sher and Addoweesh, 2012).

In this paper, the micro inverters are surveyed in a comprehensive way to present a reference on converter stages, inverter topologies, MPPT methods, isolation and operation conditions. Therefore, a detailed literature survey is performed to specify current situation of grid-connected single-phase solar inverters, research tendencies, and evolving circuit topologies and control methods. On the other hand, the design criteria of single-phase inverters are presented by considering international standards, safety regulations, and commercial products that are used in the area.

This paper is organized as follows. In Section 2, current situation of single-phase inverters and state-of-the-art are presented as a collection of device and controller configurations. The DC-DC converter stages of inverters are introduced in Section 3 with non-isolated and isolated topologies. The survey of MPPT methods that are assumed as PV side controller are analysed in Section 4 while the unfolding stage of single-phase inverters, namely grid side device topologies are given in Section 5 which is followed by inverter control methods for power regulations and grid connection requirements in Section 6, and discussions and future research anticipations are drawn in Section 7. Finally, conclusions and obtained results are presented in Section 7.

2. Single-phase inverter technologies and state-of-the-art

The solar inverters usually include an HF or LF transformer for ensuring galvanic isolation and voltage transformation ratios as seen in string inverters. Particularly, HF transformers are used to increase DC-link voltage by four or five times at the output of DC-DC converter which is supplied by a single PV module with input voltage typically ranging between 40 and 60 V in micro inverters. In addition to robust monitoring and metering capabilities, the solar micro inverters provide dedicated MPPT for each PV module differing from string inverters in a solar array. They are designed to be operated at low-power applications comparing to central and string inverters. The micro inverter

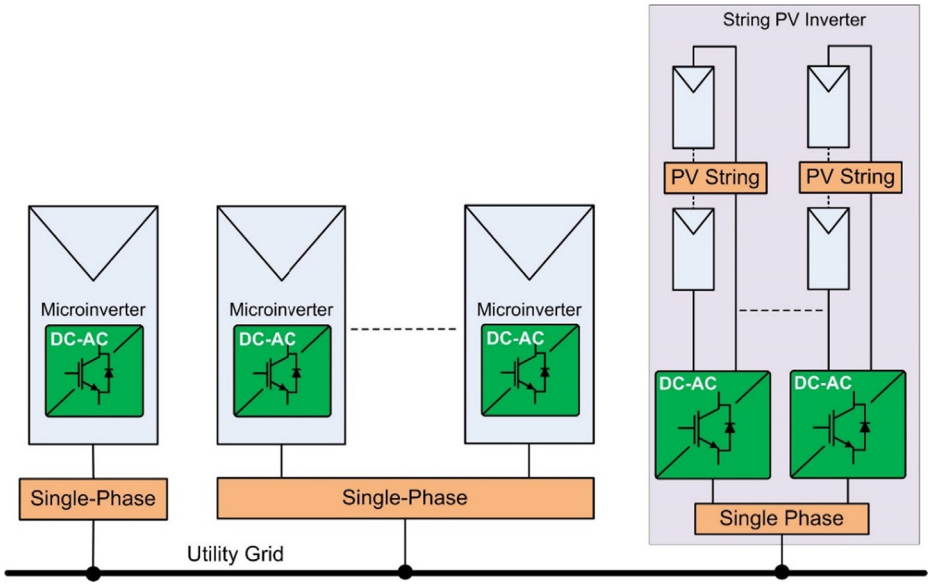

Fig. 5. Solar micro inverter configurations.

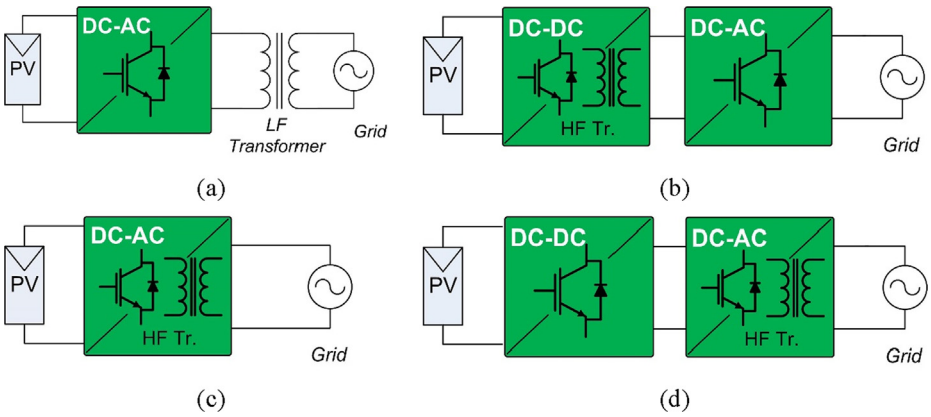

Fig. 6. Isolated micro inverter topologies, (a) LF transformer grid-tied, (b) HF transformer DC-link topology, (c) HF transformer single stage topology, (d) HF transformer two-stage topology.

configurations are shown in Fig. 5 where a string PV inverter arrangement is presented on the right hand-side of figure for comparison in terms of inverter number for each PV module. Each power converter is operated with MPPT controller at DC side of connection arrangement seen in Fig. 5 where each module has its own controller while several modules in a PV string is controlled by a single MPPT controller. Thus, the dedicated MPPT controllers increase the overall efficiency of micro inverter comparing to centralized and string inverters. However, micro inverters should tackle a number of challenging issues including its lower efficiency against string inverters (Hasan et al., 2017; Siwakoti and Blaabjerg, 2018; Zhang, 2013). The literature surveys have shown that three types of micro inverters are found as HF DC-link in single stage topology, HF two-stage topology, and single DC-link topology with two-stage configuration. Additionally, non-isolated topologies are emerging as an alternative to existing arrangements. The two-stage micro inverters are widely used due to distributed control at each stage, simple structure and low DC link capacitance (Hasan et al., 2017). The two-stage topology provides high voltage gain at DC-DC converter, easy power conversion at inverter stage and MPPT control on converter stage. The isolated topologies which are implemented by using transformers ensure voltage gain due to transformation ratios in addition to galvanic isolation as shown in Fig. 6.

The grid integration of micro inverter topology shown in Fig. 6a is performed by a LF transformer that has higher volume and size comparing to HF transformer-based topologies seen in Fig. 6b–d. The HF DC-link based topologies increase PV module voltage at DC-DC converter stage with its lower size and light weighing structure which are widely used in interleaved or flyback type device configurations (Zhang, 2013). Recently, the non-isolated topologies requiring particular interest on leakage and fault currents are paid much attention in micro inverter designs. Although there is a growing interest on transformerless micro inverters, they should comply with strict safety regulations and standards in addition to grid-connection standards. The transformerless solar inverter researches are noted in Siwakoti and Blaabjerg (2018) for decreasing leakage current and control methods such as using clamping CMV or using common ground configurations.

The device topologies that are efficient in eliminating the leakage current are listed as zero decoupled topologies including H5 and HERIC and zero-state mid-point clamped topologies as oH5, HB zero voltage rectifier (HB-ZVR). The novel inverter structures especially the resonant network configurations require increased number of switching devices and passive components increasing the cost and complexity. Moreover, high number of switching semiconductors increases switching losses due to physical state of regular silicon devices. The multilevel inverter topologies such as NPC and H4 are assumed as appropriate solutions for decreasing leakage current and THD ratios while increasing overall efficiency and power quality (Hasan et al., 2017; Siwakoti and Blaabjerg, 2018; Yahya et al., 2018).

The integration of a solar micro inverter to utility grid requires compliance to several international standards in terms of overall THD ratio, individual harmonic orders, power factor, DC current limitations, voltage and frequency deviation limits of normal and islanded operation modes, grounding and leakage current levels, and automatic synchronization. The foremost standards are IEEE 1547.1 *IEEE Standard Conformance Test Procedures for Equipment Interconnecting Distributed Resources with Electric Power Systems*, IEEE 929-2000 *Recommended Practice for Utility Interface of Photovoltaic (PV) Systems*, IEC 60364 2005 *Electrical Installations of Buildings*, UL 1741 *Standard for Safety Inverters, Converters, Controllers and Interconnection System Equipment for Use with Distributed Energy Resources*, and IEC 61000-3-2 (2001) *EMC Limits for Harmonic Emissions*. According to common concern of these standards, three types of currents should be controlled and limited which are *ground fault current* that occurs in case of insulation failure, *fault current* that denotes total utility current, and *leakage ground current* that is the resultant of capacitive parasitic components. The current control is performed by a monitoring unit measuring instant levels of fault and leakage currents (Kerekes, 2009).

Recently, zero voltage switching (ZVS) topologies have been proposed in addition to flyback or interleaved micro inverters. The ZVS topologies have been adopted to micro inverters with LC or LLC resonant converters following the DC-DC conversion stage where it comprises phase shifted full-bridge converter configuration. The LLC resonance circuit increases efficiency and power density of isolated inverter topology, and it enables use of hybrid control and modulation methods for micro inverter. As being one of the emerging micro inverter topologies, wide operation range and voltage increment opportunity are the main contribution of LCC converters. There are several different configurations proposed in the literature by improving primary and secondary side networks of HF transformer (Abdel-Rahman, 2012; Jeong et al., 2017; Jovanovic and Irving, 2016, 2015; Xingkui et al., 2016; Sun et al., 2017). The resonance network is implemented to replace conventional half or full-bridge configurations with DAB topologies that are capable to increase operating voltage range at input and at the output of DC-link.

The reminder of this section is organized to present emerging string and micro inverter topologies in threefold as non-isolated, isolated and resonant configurations. In this section, the overall device structures are presented in terms of device topology, number of active and passive devices, leakage current properties, filtering structures, and efficiency. The DC-DC converter topologies, MPPT methods, inverter topologies and control methods are presented in the following sections.

2.1. Non-isolated topologies

Although the isolated inverter topologies are accepted as an industrial standard in terms of galvanic isolation and safety requirements, the novel transformerless, namely non-isolated, inverter topologies have been proposed for decreasing implementation costs and leakage currents, and to increase the efficiency by eliminating the transformer losses. The single-phase transformerless PV inverters have become an industrial technology for a long time in grid integration of solar plants. In recent years, these string inverter topologies lower than 5 kW rated power have been widely used in low power solar micro inverters.

The most recent topologies such as H-bridge, NPC, H-NPC, HERIC, T-type, H5 and H6 are being widely used in commercial micro inverters. These configurations are designed in single-stage or two-stage structures regarding to topology and grounding requirements. A set of novel transformerless configurations for single-stage and two-stage inverters are shown in Fig. 7 (Chen et al., 2015; Kerekes et al., 2011; Meneses et al., 2013; Rojas et al., 2017; Sasidharan and Singh, 2017; Tofigh Azary et al., 2018; Vazquez et al., 2015; Xia et al., 2017). Although there is a growing interest on transformerless micro inverter topologies, they suffer from eliminating the leakage current due to parasitic capacitance that comes up from PV module through ground. The leakage current causing several concerns such as safety issues, electromagnetic interference (EMI) noises, increased THD rates, and power losses is also related with control method and CMV value. The leakage current is eliminated by using a few methods such as removing connection of PV module with utility grid during freewheeling mode, using the clamping DC-link capacitors at the input side or creating a connection between neutral of grid and negative terminal of PV module. The H5 topology which is a commercially patented configuration of recent micro inverters forces H4 section to keep the CMV constant while an additional switching device increases on-state losses two times. An improved configuration of H5 which is titled as oH5 brings an additional switching device for clamping the CMV. It is reported that the control method of this new topology requires dead-band for each switching queues to prevent short circuit of capacitors (Tofigh Azary et al., 2018; Xiao et al., 2011).

A bidirectional single-stage PV inverter which is implemented against drawbacks of aforementioned topologies is presented in Fig. 7a (Xia et al., 2017) where the dc link capacitor (C_{link}) acts as voltage source for PV MPPT. The power conversion section of this topology is based on asymmetrical half-bridge inverter while the grid-tied operation of this inverter is achieved by replacing load resistance and capacitance with grid connection. The two-way boost stage is comprised by S_1 and S_2 switches, L_b inductor and C_{link} capacitor. The input voltage V_{in} is provided by PV module while the high voltage output is obtained at V_{link} terminals. The inverter section of inverter topology is comprised by S_3 and S_4 switches, and L_{inv} inductor comprising the filter section (Xia et al., 2017).

Another recent single-stage topology proposed to decrease the leakage current is shown in Fig. 7b that is known as H-NPC where the H-bridge configuration is comprised by NPC phase branches. Each branch generates three-level output voltage, and thus the H-bridge output is obtained at five-level staircase waveform where the CMV is eliminated by the three-level pulse-width-modulation (PWM) (Rojas et al., 2017). The H-NPC topology which is used for rooftop string inverters is assumed as a reasonable solution for micro inverters since its low voltage requirement at the input and higher voltage increasing capability comparing to regular NPC topology. The dv/dt ratio over the parasitic capacitance is also decreased regarding to NPC topology that increases leakage current elimination ration of H-NPC topology.

A recent common mode transformerless inverter topology that focuses on leakage current elimination is given in Fig. 7c (Tofigh Azary et al., 2018; Vazquez et al., 2015). The proposed topology deals with creating a CM resonant network to eliminate leakage current circulating through PV module to ground (Vazquez et al., 2015). This topology is based on connecting neutral of grid with negative terminal of PV module. Therefore, a complex control method is implemented to control inverter switches S_1 and S_2 while the boost stage is controlled by using switch S_B. On the other hand, passive devices of inverter topology are comprised by capacitors C_{DC} and C_f, and inductors L_1, L_2, and L_f, and an input capacitor that requires a boost converter to obtain high voltage for MPP tracking. Despite its low number of active switches, it needs high number of passive devices that seriously decrease the efficiency.

The two-stage PV inverters comprise a DC-link between DC-DC converter and inverter stages where the fluctuations of input voltage are compensated by the converter stage. This configuration provides stable input voltage to inverter section where the oscillations caused by MPPT are decreased. The most widely used commercial topology, two-stage HERIC, is presented in Fig. 7d. The topology targets decoupling the PV module from utility grid due to control of switches S_5 and S_6 while diodes D_5 and D_6 manage the freewheeling during CM operation. A CM and differential mode (DM) voltage control method is proposed to eliminate high frequency leakage currents in Chen et al. (2015). Moreover, a complex EMI filter is comprised by using filtering inductor and capacitors to decrease parasitic components by splitting reactive elements in positive and negative terminals of grid connections.

The HERIC and H5 topologies are accepted as the most efficient and

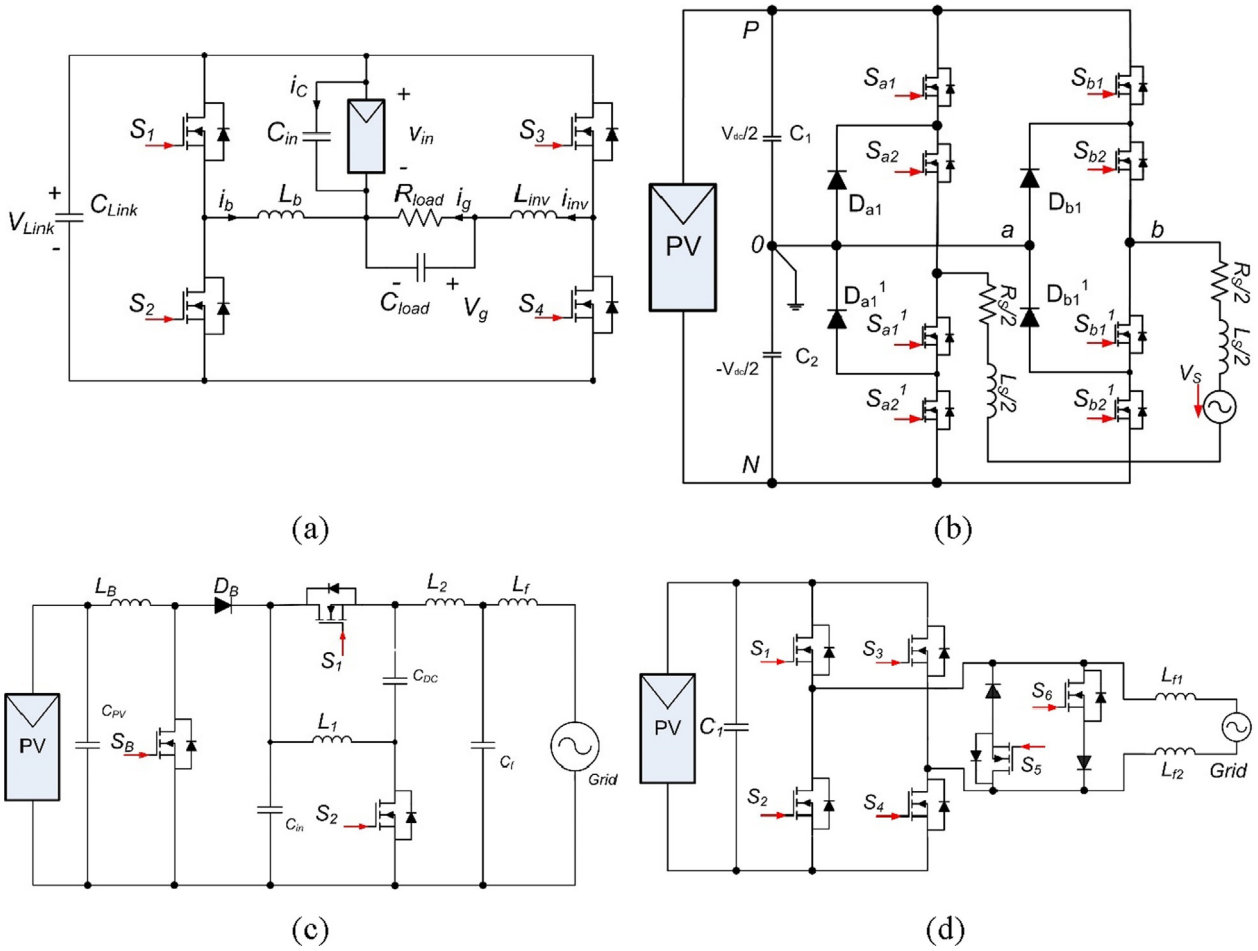

Fig. 7. Transformerless PV inverter configurations, (a) single-stage topology with minimized capacitance (Xia et al., 2017), (b) single-stage H-NPC (Rojas et al., 2017), (c) common-mode transformerless (Vazquez et al., 2015), (d) two-stage HERIC inverter.

leading configurations decoupling solar arrays and utility grid. The derivatives of HERIC topology are H5 and H6 that are comprised by five or six switching devices as their name imply (Chen et al., 2015; L. Zhang et al., 2014). HERIC topology provides the least switching loss among other topologies under hard switching conditions. In Chen et al. (2015), it is noted that a single-phase transformerless HERIC inverter with SiC JFETs can provide 99% peak efficiency. While it is expressed that peak efficiencies of H5 and H6 inverters can be increased up to 98%, these topologies are not still able to cope with some drawbacks such as higher volume of passive components, decreased efficiency at high switching frequencies, and high frequency common-mode voltage (Chen et al., 2015; L. Zhang et al., 2014; Xiao et al., 2017, 2015). The H5 topology is comprised by an additional switch to conventional H4 topology that decouples PV module from grid when the inverter output voltage is at zero. Thus, the leakage current is prevented. The HERIC topology which is improved with similar idea required two additional switches at the output of H4 inverter while H6 employs additional switches at the input stage of inverter.

Zhange et al. compared three recent topologies in terms of leakage current levels under same operation conditions in Chen et al. (2015) that H5 topology draws the least leakage current at 6 mA while others draw around 9 mA. On the other hand, The European efficiencies of H5, H6, and HERIC topologies are determined at 96.78%, 97%, and 97.09%, respectively. Although the HERIC topology presents highest efficiency among others, it suffers from leakage current level.

2.2. Isolated topologies

As discussed earlier, the CMV and CM current cause to several issues in terms of safety, EMI noises, increased THD ratios and other power quality deficiencies in transformerless topologies. There is a wide interest on isolated topologies including novel DC-DC converter topologies and inverter configurations in order to minimize parasitic and disturbing drawbacks seen in transformerless device topologies. It is also widely accepted that isolated topologies present higher reliability and galvanic isolation comparing to transformerless topologies by eliminating the CM disturbances. The main contribution of isolated micro inverter topologies is galvanic isolation between PV module and utility grid that facilitates decreasing the leakage current level in CM where special requirements exist in non-isolated topologies. The HF isolation transformer ensures the galvanic isolation at the DC-DC converter section (Öztürk et al., 2018).

The single-stage isolated topologies are comprised by regular flyback or interleaved flyback converter topologies while the multi-stages include a wide variety of DC-DC converter and inverter topologies in a single device configuration. The main sections are comprised by a booster converter and by a power conditioning inverter in multi-stage micro inverter structure. The two-stage or multi-stage topologies provide power decoupling and MPPT control at the first stage while active and reactive control with grid connection are performed at the output stage. The list of recent isolated micro inverter topologies are presented in Fig. 8.

The power conversion of PV module is performed by single-stage or multi-stage configurations as shown in Fig. 6 where one or more stages

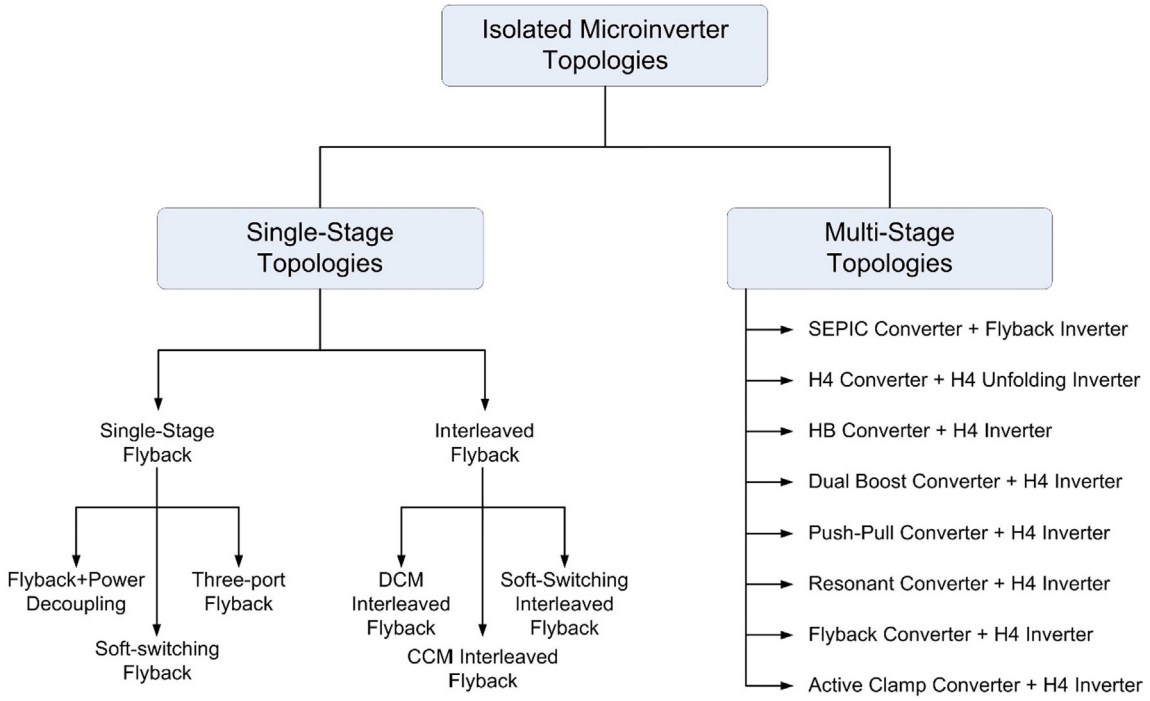

Fig. 8. Isolated micro inverter topologies.

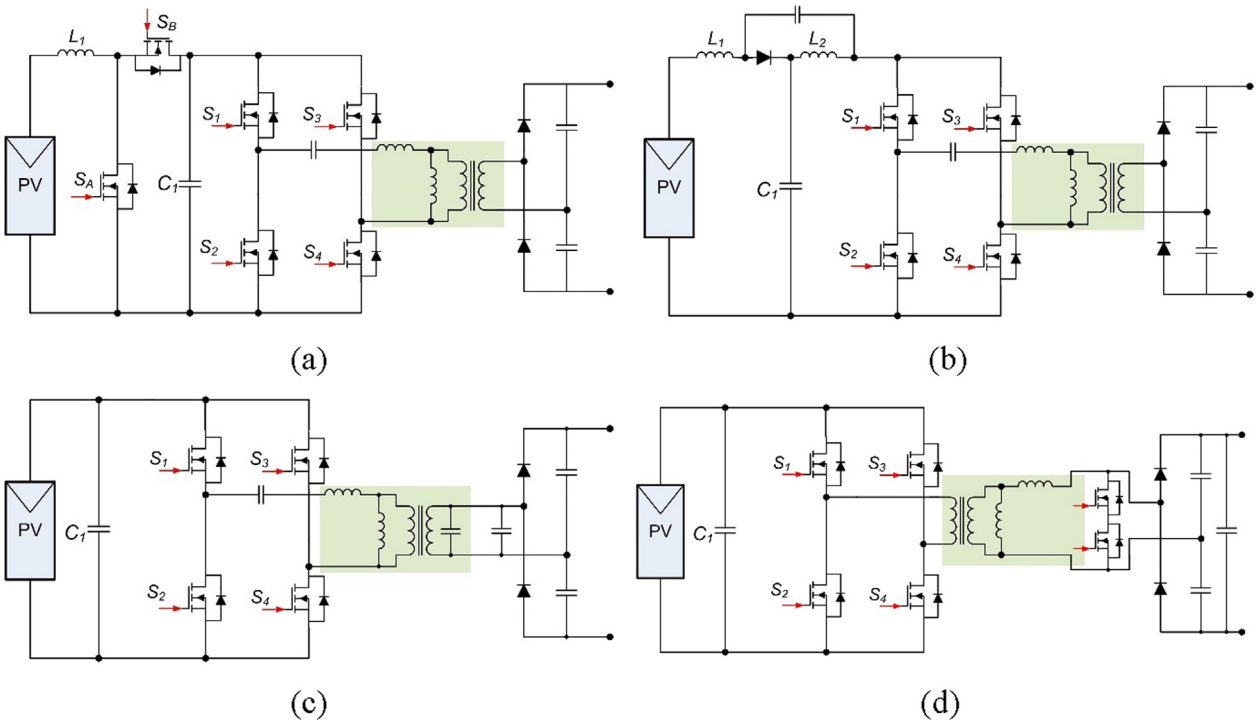

Fig. 9. The emerging resonant micro inverter topologies, (a) two-stage topology with synchronous boost and series-resonant converter, (b) quasi-Z source series resonant converter, (c) LLCC series-parallel resonant converter, (d) series resonant converter with bidirectional switch.

are employed to increase DC-link voltage in multi-stage topologies. The HF transformers can be located at DC-DC converter section of single-stage topologies while it can be coupled at DC-DC converter stages or at inverter section of multi-stage configurations. The single-stage isolated converters are fundamentally improved by using flyback or interleaved topologies as expressed on the left side of Fig. 8. Both configurations can be implemented with regular topologies, soft switched resonant topologies or three-port topologies while the multi-stage topologies are widely inherited from conventional H4 structure at inverter section. The SEPIC, push-pull, flyback, resonant, active clamp converter topologies are commonly used in DC-DC converter sections of multi-stage micro inverter topologies (Hasan et al., 2017).

The DC-link between converter and inverter stages accommodates high-voltage by decreasing decoupling capacitor requirement. This voltage increasing stage is comprised by using center-tapped transformer in single stage topologies. The recent isolated topologies are

developed with center-tapped transformer in single stage or flyback DC-DC converters that are followed by a half-bridge or full-bridge inverters.

The detailed presentation of isolated single and multi stage topologies are presented in the next section under DC-DC converter topologies. Moreover, the resonant converter and micro inverter topologies are discussed in the following part.

2.3. Resonant topologies

The DC-DC converters can be classified into two categories as hard switching or PWM converter and resonant converters. The recently presented topologies belongs to PWM converter configuration since they do not require any inductor or capacitor tank circuit for managing the switching operation.

However, resonant converters are comprised with additional L-C networks controlling the charge and discharge cycles of energy transfer. The resonant converters are commonly configured with HF transformers providing the galvanic isolation. The leakage inductance of HF transformer causes additional voltage stress on switching devices and increases switching power losses of PWM converters while this stress is eliminated by tank circuit of resonant converter. In addition to decreasing switching losses, the resonant converters are implemented in less size and weights due to increased switching frequency capability that decreases component sizes, and it creates a suitable intermediate converter infrastructure between PV module and inverter stage.

The DC-DC converter stage of a PV inverter is fundamentally required to adapt output voltage of PV module to interface inverter stage by the MPPT control algorithm. The galvanic isolation requirement prevents increasing the switching frequency due to resultant increased leakage inductance and increased EMI noises in hard switched converter topologies. Therefore, the hard switching topologies are combined with resonant tank circuits to overcome these drawbacks. One of the combinational circuit topologies is shown in Fig. 9a that is comprised by a conventional synchronous boost converter and a series resonant DC-DC converter (SRC). The SRC provides high efficiency with eliminating switching losses due to ZVS or zero current switching (ZCS) methods. The bidirectional power flow and core excitation enables SRC to have high power density comparing to conventional isolated topologies. A single stage DC-DC converter can be implemented by replacing boost converter with an impedance networks as depicted in Fig. 9b which is known as quasi impedance source (qZS) SRC. The Z source network is comprised with capacitors, inductors, and diodes in a featured configuration. The Z circuit acts as a short circuit to boost the input voltage along the input terminals of SRC, and the input voltage supplied by PV module is preregulated at this stage. The operation modes of qZS network are defined as shoot-through and non-shoot-through regarding to charge and discharge cycles of inductors. The shoot-through mode defines the charging cycle of inductor where the diode is open circuit while the load is supplied with the charge of inductors and capacitors in non-shoot-through cycle (Kabalci, 2018; Kouro et al., 2015).

The single-stage inverters are also implemented in multi-resonant topologies in order to improve short-circuit immunity and operation voltage range with high efficiency. Such an inverter topology that is known as LLCC series-parallel resonant converter is shown in Fig. 9c. The output network of LLCC converter is also followed by a voltage doubler rectifier (VDR) circuit. On the contrary of its complex resonant and output networks, it includes minimum number of active devices where series and parallel resonance devices are essential in decreasing leakage inductance. According to a comparison table of emerging resonant converter topologies, the DC-DC converters with series resonance networks provide highest efficiency with 97.4% while parallel topologies provide 96.6% at peak efficiency (Vinnikov et al., 2017).

There are several resonant converter topologies have been proposed by integrating regular boost and LLC resonant converters in literature. A number of dual-mode resonant converters with single stage H4 topologies are presented in Hasan et al. (2017) where primary side is comprised as shown in Fig. 9d. The switching losses of single-stage primary side are decreased with resonant network and bidirectional switches that are located before VDR section of micro inverter configuration. The switching frequency of such a resonant converter is increased up to 1 MHz range which decreases switching losses and inductance leakages while increasing the overall efficiency up to 97.6% (Hasan et al., 2017). The LLC resonant converters are usually operated at varying switching frequencies to compensate input voltage and load changes. It is noted that the duty cycles applied to switching devices are kept around 50% and dead band is applied between *on-off* transitions to prevent switching losses in ZVS control.

The switching frequency range which is determined by magnetizing inductance L_M of transformer depends to variation of input voltage for ensuring more flexible operation. However, wide range of switching frequency causes adverse effects on performance and efficiency of converter. The magnetizing inductance determines a path for resonant current during very low or zero load operations where the decreasing L_M provides decrement on switching frequency and thus, converter acts like a parallel resonant device under no load operation (Jovanovic and Irving, 2016).

3. Recent DC-DC converter topologies used in solar inverters

A typical solar inverter is located between PV module and utility grid where it converts the harvested energy to AC waveform. The isolated topologies are widely used to meet safety requirements and to eliminate the effects of leakage currents in grid-connected infrastructure. As expressed earlier, the isolation is achieved by using an HF transformer that provides classification of topologies with the name of DC-link, pseudo-DC link, and high frequency. It is noted that pseudo-DC link topology provides higher efficiency comparing others due to its single stage structure (Hu et al., 2012). The micro inverter which provides power conversion through utility grid should comply with lifespan of a PV module that is around 25 years. Therefore, the devices and components of solar inverter are required to be long-life and equipped with control methods improving the reliability and efficiency of micro inverter. The DC-DC converter section plays crucial role in two-stage micro inverter topologies since it is the vital stage on regulating the fluctuating PV voltage. Some technical challenges faced in DC-DC converter stage are related with wide operating voltage at input, wide input power rate due to fluctuating irradiation and temperature effects, increasing power density which is required due to increment of PV module power, and high efficiency demand (Hu et al., 2012; Zhang, 2013).

These requirements are met using an intermediate storage element which is mostly a capacitor coupled between DC-DC converter and inverter stages. The electrolytic capacitors are usually chosen for intermediate dc bus due to their operating lifetime ranging between 1000 and 7000 h. The operating voltage and required capacitance are determined according to usage section as input or output capacitor as shown in Fig. 10. In case of input capacitor used for low voltage input

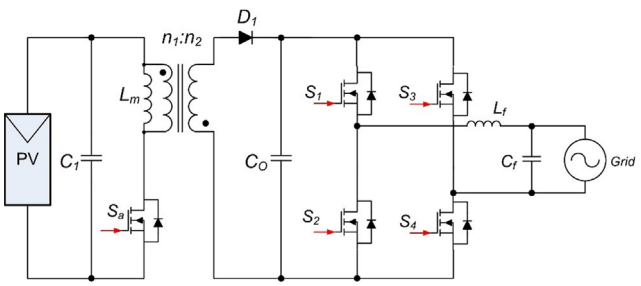

Fig. 10. Circuit diagram of a conventional flyback converter for solar micro inverter.

which ranges around 25 V to 55–60 V for PV modules, the capacitance should be selected high enough to decrease input voltage ripples (Hu et al., 2012).

There are a wide variety of micro inverters proposed in literature which are implemented for supplying MPPT control, voltage amplification at DC stage, output current and voltage control, and galvanic isolation. Although many DC-DC converter topologies such as half-bridge, conventional boost, resonant converters and DABs have been proposed in literature, the flyback and interleaved converters come forward as the most recent ones among others. On the other hand, combination of both topologies, namely interleaved flyback arrangements are assessed as emerging novel topologies due to their improved circuit configuration and control methods. The higher step-up capability of these topologies meets the robust voltage increasing requirements of micro inverters since the input voltage yielded from PV modules are generally between 40 V and 60 V. Moreover, HF transformer configuration enables to operate at high switching frequency with the aid of resonant devices besides galvanic isolation (Rezaei et al., 2016; Zapata et al., 2016). The conventional flyback converter that is followed by an H4 inverter stage is one of the most common micro inverter topologies in industry. The device configuration is shown in Fig. 10 where the HF transformer is used to create a galvanic isolation between input and output of converter stage while the conversion ratio of transformer supplies higher voltage elevation capability to converter.

The converter topology and conversion ratio of transformer enable flyback converter to operate as a conventional buck-boost device with increased voltage gain that is defined as follows where D denotes duty cycle ratio;

$$V_O = \frac{n_2 \cdot D}{n_1 \cdot (1 - D)} V_{PV} \tag{1}$$

A conventional flyback topology combined in interleaved structure to comprise a single-phase inverter is illustrated in Fig. 11 where the decoupling capacitors are located at the input and output sections of converter, and an unfolding inverter stage is comprised in H4 topology. The surveyed topology which is originally proposed in Rezaei et al. (2016) is improved by adding active clamping switches for analysing discontinuous conduction mode (DCM) and boundary conduction mode (BCM) operations of converter section. It is noted in International Electrotechnical Commission and Oruganti (2014) that flyback converter draws lower peak currents during continuous conduction mode (CCM) that ensures higher efficiency for dc converter and inverter stages. The flyback topology is assumed as a proven configuration in terms of efficiency and reliability with its decreased switching device numbers. Sukesh et al. proposed to decrease switching losses caused by hard-switching methods by operating the flyback converter with ZVS control methods particularly during high frequency operations (Sukesh et al., 2014).

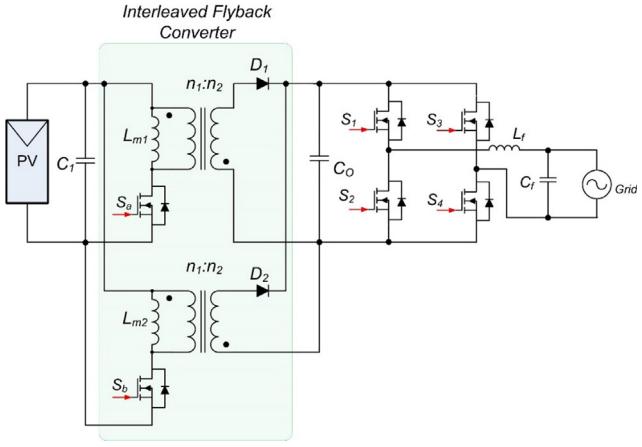

Fig. 11. Circuit diagram of an interleaved flyback single-phase inverter.

The flyback topology operates as a voltage source which is not affected by load changes in CCM mode due to its magnetizing inductance at HF transformer seen as L_{m1} and L_{m2} in Fig. 11. The center-tapped transformer and two-way switching devices have been conducted on the grid side of proposed ZVS controlled converter in Sukesh et al. (2014). Another flyback converter topology ensuring CCM operation with open-loop controller on primary side of HF transformer has been proposed in International Electrotechnical Commission and Oruganti (2014). The micro inverters based on flyback topologies are also described as module integrated converters (MICs) and flyback MIC (FMIC) which are proposed in different configurations and control methods in Edwin et al. (2014), Thang et al. (2014).

The preliminary literature survey exhibits that the DC-DC converter topologies of micro inverters are much more sophisticated comparing to conventional non-isolated topologies. The improvements of resonant converters and increased availability of centre-tapped HF transformers have leveraged development of recent converter topologies. Although they would be improved in ZVS, resonant or push-pull topologies, they are based on two fundamental topologies as flyback and interleaved configurations (Baka et al., 2019; Feng et al., 2019; Hasan and Mekhilef, 2017; Tayebi et al., 2019; F. Wang et al., 2018; Zeb et al., 2018; Zhang et al., 2018, 2019).

3.1. Flyback DC converter

One of the earliest sensorless flyback converter for PV power systems has been proposed by Kasa et al. with a centre-tapped secondary winding transformer as shown in Fig. 12 (Hasan et al., 2017; Kasa et al., 2005). The flyback converter was not widely preferred when it has been first proposed in the literature since there had not been much familiarity. However, the unique configuration of flyback topology was eliminating the additional converter requirement and was able to convert any DC power level to ac at the output. The main device topology is quite simple to build and required number of semiconductors has been drastically decreased comparing to any other topology. Moreover, flyback topology provides better electrical potential due to its isolation feature between PV module and grid connection (Kasa et al., 2005).

Shimizu et al. proposed a flyback-type PV converter to overcome partial shading and lifetime issues of electrolytic input capacitor (Shimizu et al., 2006). The proposed device configuration was based on replacing electrolytic capacitors with film capacitors at small values, and transmitting the stored energy to output over centre-tapped secondary windings. Hu et al. proposed two different three-port flyback converter for PV micro inverters where the circuit configurations are illustrated in Fig. 13a and b (Hu et al., 2013, 2012). The first topology seen in Fig. 13a is improved to decrease effects of large capacitance requirements in power decoupling of PV micro inverter.

The proposed topology which is called three-port flyback converter is comprised in a novel integrated configuration with single-stage

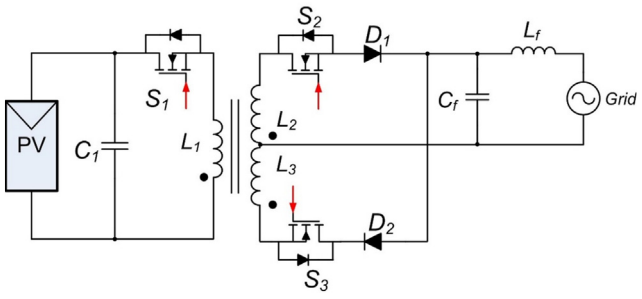

Fig. 12. Single stage flyback micro inverter with centre-tapped secondary transformer.

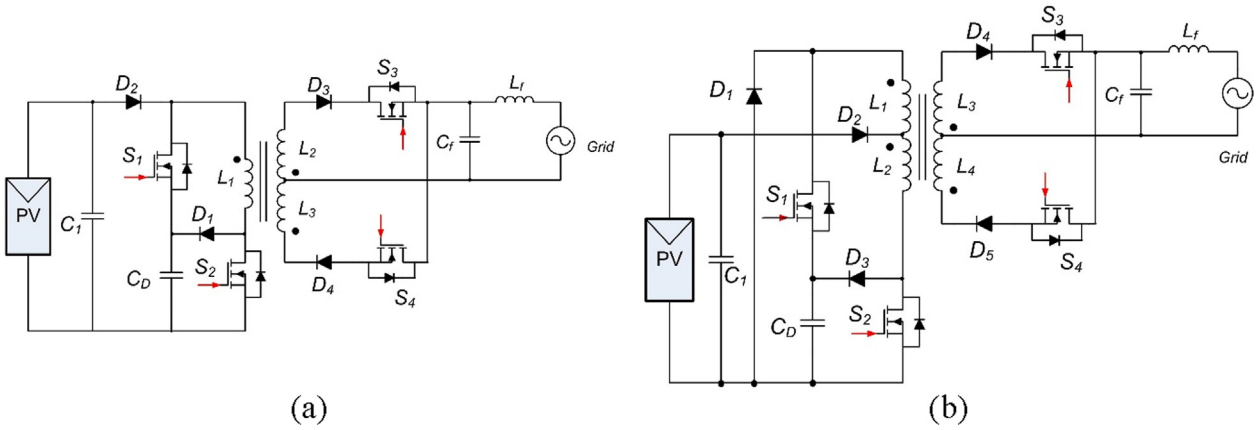

Fig. 13. Three-port flyback micro inverters (a) without using electrolytic capacitors (Hu et al., 2013) (b) with power pulsation decoupling capability (Hu et al., 2012).

power conversion and power decoupling features. This results in reduced component number, compact power stage, low cost, and increased efficiency (Hu et al., 2013).

The three-port flyback converter topology is improved by using conventional topology where an additional switch S_2 and a diode D_2 are used to realize the power decoupling function at the primary side in Fig. 13a. The two-winding secondary is used to generate ac output voltage depending to line frequency operation of two switches S_3 and S_4 in series with diodes D_3 and D_4, respectively. The decoupling capacitor C_D is located at the primary side to prevent double line-frequency stress at the PV module section. The difference of excessive input power which is higher than output power is charged to decoupling capacitor while the deficit power in case of higher output power required is met by discharging the decoupling capacitor. In this case, the discharge of decoupling capacitor is ensured by turning *on* the switch S_2 and required additional power is inherited to increase output power. Therefore, there are two operation modes exist for this converter where the first one is the charging mode while the second one is the discharging mode (Hu et al., 2013).

Hu et al. proposed a novel topology seen in Fig. 13b that is based on the previous one to improve power decoupling capability of single stage flyback configuration. In addition to its power decoupling capacity, the capacitor C_D is used as a snubber capacitor for recycling the leakage energy generated by primary of transformer. The additional diode D_2 is included to prevent reverse current flow of power decoupling capacitor to PV module in this topology while diode D_3 provides a leakage current discharge path in the lower loop (Hu et al., 2012).

In addition to decoupling circuit improvements on primary side, some other studies have proposed novel topologies placing decoupling circuits at secondary side of flyback converter. Such topologies are defined with the names of active clamp converters and HF ac link flyback converters as conducted in Hasan et al. (2017). These kinds of novel topologies are focused on replacing electrolytic capacitors with long life film capacitors and providing an active decoupling or clamping network on primary or secondary side of HF transformer. In addition to flyback converters, the interleaved and interleaved flyback topologies are also proposed in the literature for providing long life and reliable micro inverter topologies.

3.2. Interleaved flyback DC converter

It is noted in Edwin et al. (2014) that inverter failures are related to reliability of components and switching devices in terms of lifetime and operational capabilities. The double-frequency decoupling capacitor which is concluded earlier is one of the most important components limiting the lifetime of entire micro inverter. Besides the flyback topologies replacing electrolytic capacitors with film capacitors, improved interleaved converters have been proposed for increasing the efficiency and power density with the name of MICs in literature. Edwin et al. presented a detailed review on MIC topologies and control methods in Edwin et al. (2012) which is focusing on DCM, CCM and BCM operation modes of converters in PV applications. The expressed study classifies MIC topologies according to DC-link availability, switching device numbers, soft switching methods, and decoupling capacitances.

However, it is well known that flyback inverters behave as a current source in DCM operation and it will cause higher current stress on primary side of HF transformer that drastically decreases efficiency of micro inverter. On the other hand, the flyback topology itself provide a little higher efficiency in CCM operation mode due to its lower electromagnetic interference (EMI), decreased current stress on primary side and lower operating voltage comparing to DCM mode. The CCM operation is ensured by precisely controlled duty cycle of switching devices preventing the saturation of magnetizing inductor at transformer. The transition between DCM and CCM is known as BCM which is proposed by some researchers to be taken into consideration to overcome aforementioned drawbacks (Dong and Tian, 2017; Edwin et al., 2014; Lai, 2014; Lodh et al., 2016; Zhang et al., 2013a).

There are some literature outcomes expressing that the flyback converters operate as current source regarding to peak-current control methods in BCM mode. It is also possible to increase overall efficiency by eliminating the diode losses occurred in reverse-recovery and applying ZVS control to flyback converter. The main issue in flyback converter is the increment of primary current while the output current decreases which is caused since the DCM and BCM modes are used together in control. Eventually, the flyback micro inverter should be operated in DCM mode around zero-crossing points of grid voltage for decreasing the switching losses and should be operated in BCM mode during the other points to increase overall efficiency (Dong and Tian, 2017; Zhang et al., 2013a). The single-stage flyback converters which are developed by adding an unfolding inverter at the grid side connection are novel solutions owing to their simple control, high power density and high voltage increment features. However, the limitations on magnetic devices and HF transformers force researchers to discover novel topologies and device configurations with or without magnetic devices. The ZCS is another control method which is applied for DCM and BCM operation modes of micro inverters (Lai, 2014; Lodh et al., 2016).

The power range of a flyback micro inverter is increased by connecting several flyback converters in parallel to comprise an interleaved flyback configuration. A sample device topology is shown in Fig. 14a where two-phase interleaved structure is followed by an unfolding inverter bridge at the utility grid side. This device topology is proposed by Zhang et al. for investigating the interleaved flyback micro inverter in

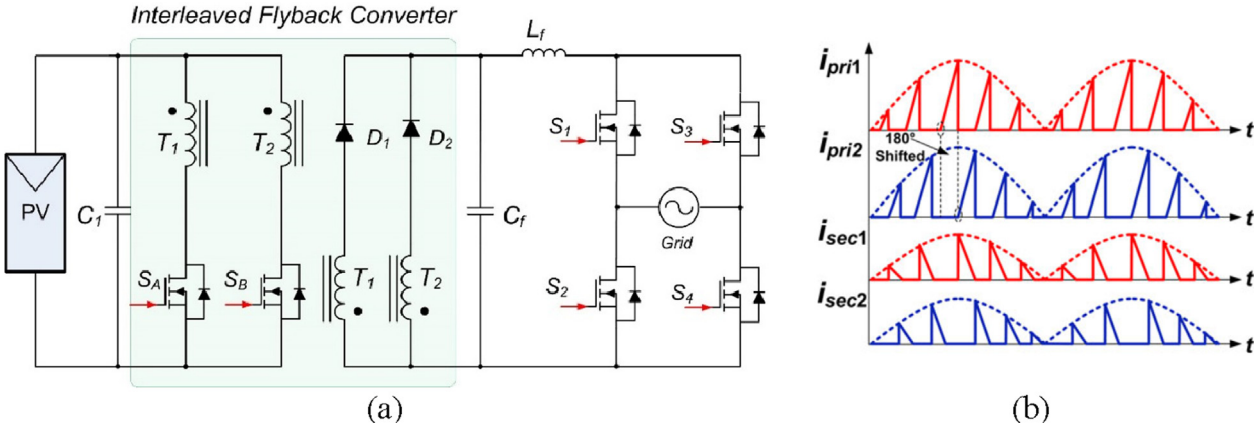

Fig. 14. Two-phase interleaved flyback micro inverter topology, (a) circuit diagram, (b) current waveforms of the interleaved flyback inverter (Zhang et al., 2013b).

BCM and DCM operation modes at different load conditions and loss situations. The performed analyses have proved that DCM control strategy provides higher efficiency over BCM mode up to 200 W rated power. The two-phase interleaved flyback micro inverter brings the advantages on ensuring the current and power sharing, and decreasing the current stress on primary side by managing conduction orders of each phase. The decreased losses of switching transitions, transformer core, and driving devices gradually increase the overall efficiency of converter.

The current waveforms of interleaved flyback converter are shown in Fig. 14b where each phase is shifted at 180° to ensure current sharing and isolated conduction control (Zhang et al., 2013b). The unfolding inverter section is comprised by a CSI configuration where switches S_A and S_B act as main switching devices at the primary side while diodes D_1 and D_2 provides rectification on the secondary side of transformer. The loss distribution analyses have been performed according to both operation modes as shown in Table 2 where the converter has been controlled under 36–60 V input voltage, 220 V_{AC} output voltage and at 100 kHz switching frequency. The highest share of losses has been indicated with bold in the list.

The test outcomes prove that DCM operation mode draws seriously less losses in terms of turn-off power losses and gate driving circuit losses while core losses are slight lower than BCM mode. The presented analyses have also shown that the two-phase interleaved flyback converter provides higher efficiency under light loads comparing to single-phase flyback micro inverter topology (Zhang et al., 2013b).

There are several other topologies have been derived from combination of interleaved and flyback converters that are listed in Hasan et al., 2017; Kim et al. (2013), Meneses et al. (2015), L. Zhang et al. (2014), Z. Zhang et al. (2014). However, all the topologies are improved regarding to developing control methods and active clamping features of the micro inverter configuration in Fig. 14. The control methods are related with MPPT controller on dc stage and synchronization control on inverting stage.

Table 2
Loss analysis of two-phase interleaved flyback micro inverter in DCM and BCM modes (Zhang et al., 2013b).

	DCM		BCM	
	Loss (W)	Percentage (%)	Loss (W)	Percentage (%)
Turn-off power loss	**0.8**	18.3	**2.50**	31.5
Gate driving loss	**0.83**	18.9	**2.83**	35.7
Mosfet power loss	0.60	13.7	0.40	5.04
Core losses	**0.84**	19.2	0.99	12.5
Copper losses	0.71	16.2	0.89	11.2
Diode power losses	0.6	13.7	0.32	4.04

4. Maximum power point tracking methods

MPPT is an essential control algorithm to detect the maximum input power corresponding to fluctuations on source voltage and current. Although the MPPT algorithm targets to maximize efficiency, it will not properly work if both stable and varying conditions are not tracked. The overall efficiency of a power conversion system is depended to considering all changes on source and load variations. Therefore, an MPPT algorithm that is used to improve efficiency of a PV system should consider the changes on operating circumstances. There are a lot of fundamental and derivative MPPT methods proposed in the literature (Kabalci, 2017; Moon et al., 2015; Romero-Cadaval et al., 2013). The main difference on MPPT algorithms are classified into two main groups that are defined as direct MPPT and indirect MPPT methods. The direct methods are operated by detecting PV voltage, current, and/or power while indirect methods are based on calculation of PV voltage or current at the maximum power point.

The direct methods are faster in detection and response quickly to fluctuations since they are based on measurements instead of calculations. The most widely known and used MPPT methods are perturb-and-observe (P&O) and incremental conductance (InCon) MPPT algorithms among others. The commercial PV inverters are also based on these direct and perturbative algorithms due to their faster response and reliable operation. Some MPPT algorithms have been improved by using computational algorithms as fuzzy logic control (FLC), artificial neural network (ANN), particle swarm optimization (PSO), and genetic algorithm (GA). Although the computational methods provide better analytical calculations, they are mostly very complicated and require higher system performance. On the other hand, direct algorithms can be modified to obtain global MPPT operation in addition to local MPPT detection (Kabalci, 2017; Romero-Cadaval et al., 2013).

The constant voltage MPPT, open-circuit MPPT, and short-current pulse-based MPPT algorithms are widely used indirect algorithms due to their simplicity. These are based on calculations of the parameters such as system voltage, open-circuit voltage, short-circuit current as their name imply. The operating voltage is depended to PV temperature, and seasonal changes affecting the reliability. Furthermore, these algorithms lack on reliability due to aging and pollution of PV modules. Many MPPT methods have been compared to detect design criteria as shown in Table 3.

The indirect MPPT methods are not true MPPT and indeed, the measured values of open circuit voltage, constant voltage, and short-circuit pulse-based algorithms are based on calculated parameters instead of measurement. Therefore, the response time of these MPPTs are lower than direct or computational MPPT algorithms. On the other hand, computational algorithms require complex mathematical operations and high precision microprocessors to operate predefined iterations. This kind of MPPT control is achieved by using high cost

Table 3
Comparison of widely known MPPT methods.

MPPT Method	True MPPT	Array Based	Response Time	Complexity	Measured Values
Perturb-and-Observe (P&O)	Yes	No	Variable	Low	Voltage, Current
Incremental Conductance (InCon)	Yes	No	Variable	Medium	Voltage, Current
Sliding Mode	Yes	No	Fast	Medium	Voltage, Current
Capacitor Control	No	No	Medium	Low	Voltage
Load I-V Control	No	No	Fast	Low	Voltage, Current
Open-Circuit Voltage (V_{OC})	No	Yes	Medium	Low	Voltage
Constant Voltage (CV)	No	Yes	Medium	Low	Voltage
Short-Circuit Pulse-Based (I_{SC})	No	Yes	Medium	Medium	Current
dP/dV and *dP/dI* feedback	Yes	No	Fast	Medium	Voltage, Current
Fuzzy Logic Control (FLC)	Yes	Yes	Fast	High	Variable
Artificial Neural Network (ANN)	Yes	Yes	Fast	High	Variable
Particle Swarm Optimization (PSO)	Yes	Yes	Fast	High	Variable
Genetic Algorithm (GA)	Yes	Yes	Fast	High	Variable

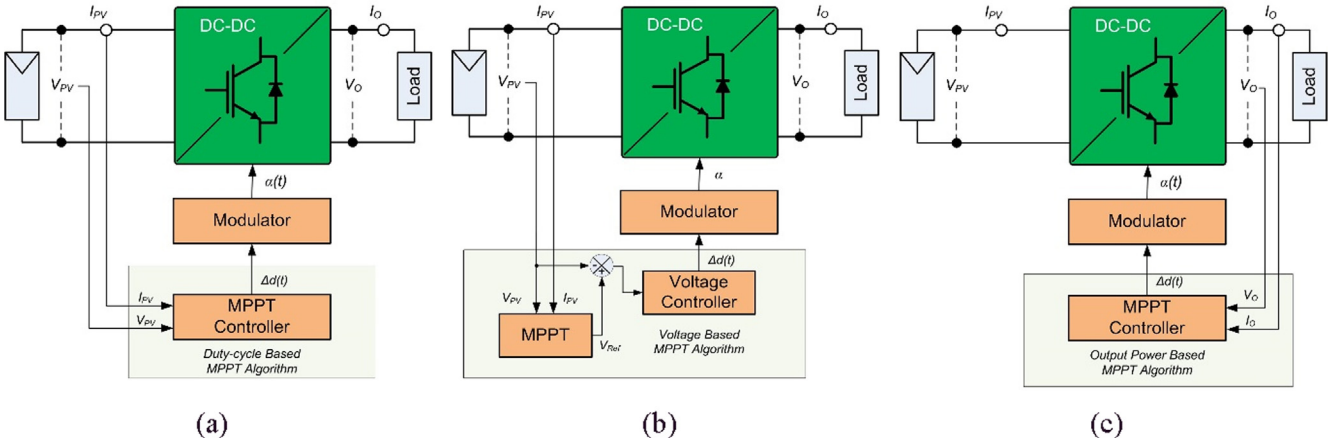

Fig. 15. MPPT algorithms, (a) duty cycle based (b) reference voltage based (c) output power based.

hardware. Feed forward or feedback control algorithms including capacitor control, *dP/dV*, *dP/dI*, and load *I-V* MPPTs comprise another category. These methods mostly do not require voltage and current measurement of solar array and can provide better performance by integrating to existing methods (Furtado et al., 2018; Kabalci, 2017; Li et al., 2018; Montoya et al., 2016).

The MPPT software can be classified into three groups regarding to input parameters detection as duty cycle based, voltage based, and output power-based algorithms as shown in Fig. 15. The MPPT algorithms are mostly based on solar array voltage due to their dependence to irradiation. The regular direct MPPT algorithms perform control operations with duty cycle or voltage-based configurations as shown in Fig. 15a and b, respectively. Another MPPT configuration with DC-DC converter is performed by using output power or feedback based algorithms as seen in Fig. 15c (Kabalci, 2017; Romero-Cadaval et al., 2013). Although the MPPT algorithms target to maximize yielded energy, they are unable to detect the difference on local MPP (LMPP) and global MPP (GMPP) under partial shading circumstances that are caused by effects of clouds, buildings, dust, and trees. Therefore, regular MPPT methods lack to response under partial shading and load variations. A number of GMPPT algorithms have been proposed to address partial shading problems (de Brito et al., 2013; Furtado et al., 2018; Li et al., 2018). These methods require additional circuits and complex mathematical operations and the most widely known ones are based on soft computing and optimization algorithms.

The requirements cause hindrances for commercial PV systems by increasing costs due to high performance microprocessors, additional sensor and circuit devices, and increased convergence times. The improved MPPT methods have been enhanced by taking into consideration of DC-DC converter output voltage since it is drastically decreased under partial shading conditions. This approach is proposed as an alternative to GMPPT algorithms such as 0.8 V_{OC}, reduced voltage range, and PSO methods (Ahmed and Salam, 2017; Chen et al., 2014; Furtado et al., 2018; Li et al., 2018). The MPPT methods are also adapted

Table 4
Widely used MPPT methods (Çelik et al., 2018).

Offline MPPT Methods	Online MPPT Methods	Hybrid MPPT Methods
Short Circuit Current	Perturb-and-Observe (P&O)	Analytical Calculation and P&O
Open-Circuit Voltage (V_{OC})	Incremental Conductance (InCon)	Particle Swarm Optimization (PSO)
Look-up Table	Sliding Mode	Genetic Algorithm
Fuzzy Logic Control (FLC)	Capacitor Control	Optimized FLC
Artificial Neural Network (ANN)	Load I-V Control	P&O and ANN
Genetic Algorithm (GA)	Ripple Correlation Control	Differential Evolution
Constant Voltage (CV)	Forced Oscillation	Direct Prediction Method (DPM)
Short-Circuit Pulse-Based (I_{SC})	*dP/dV* and *dP/dI* feedback	
Temperature Based Method		

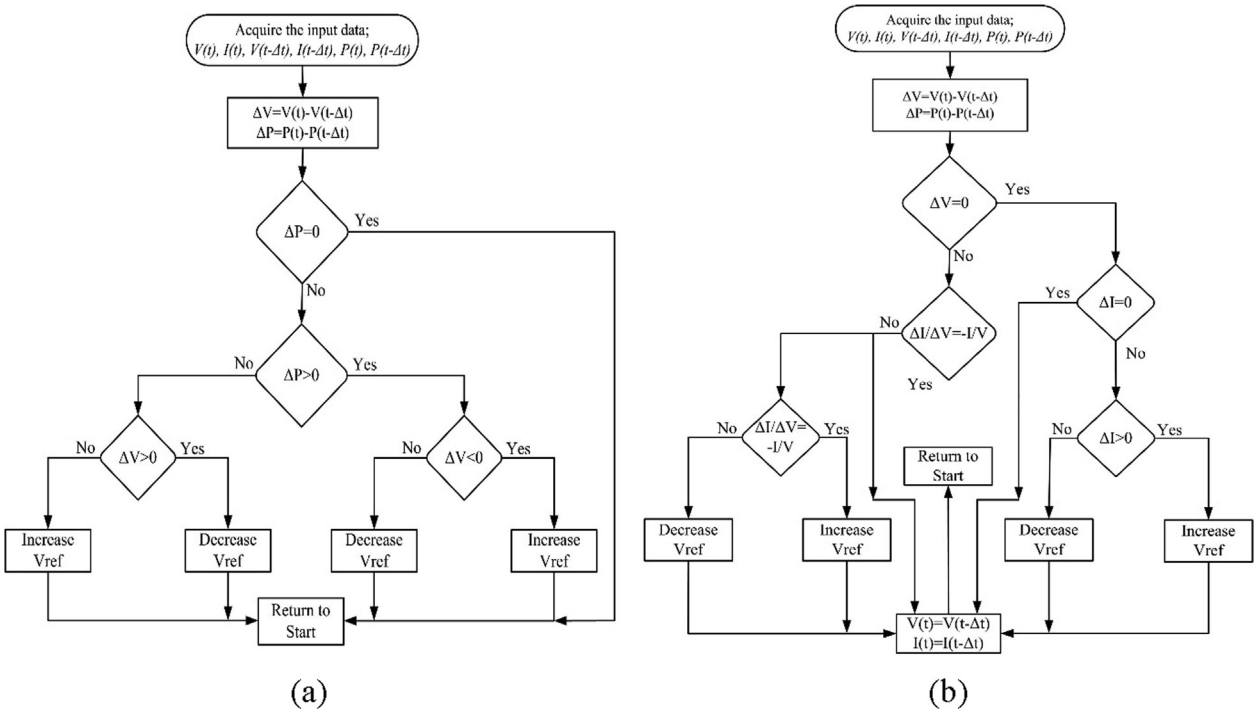

Fig. 16. Flowchart of two conventional MPPT algorithms, (a) P&O, (b) InCon (Kabalci, 2017).

according to requirements of micro inverters in terms of power decoupling and control features.

4.1. Conventional MPPT algorithms

Although the MPPT control could be applied to inverter stage, it is mostly used for control of dc converter stage in micro inverters. Celik et al. have presented a comparison table in Çelik et al. (2018) where MPPT methods are classified as offline, online and hybrid methods which are shown in Table 4.

The most widely used conventional MPPT methods are based on P&O and InCon algorithms where PV voltage and current are instantly measured and processed in a comparison algorithm to detect derivation of power. These algorithms are based on detecting whether the operating point of the load is on the right-hand side or on the left-hand side of MPP regarding to following equations. In case the deviation of power is greater than that of voltage, this means the power curve is hill-climbing and thus, it is required to increase duty cycle rate as seen in (2) while vice versa for decreasing ratio of power to voltage deviation as given in (3).

$$\frac{\partial P_{PV}}{\partial V_{PV}} < 0 \Rightarrow M = M - \Delta M \tag{2}$$

$$\frac{\partial P_{PV}}{\partial V_{PV}} > 0 \Rightarrow M = M + \Delta M \tag{3}$$

The flowchart of P&O and InCon MPPT algorithms are presented in Fig. 16a and b respectively. The linear control methods lack on harvesting available maximum power from PV module since it draws a nonlinear characteristic in power-voltage curve. There have been several studies presented in literature for conventional methods. The improved processor capabilities have overcome the convergence speed, dismissed MPP tracking and partial shading deficiencies of conventional methods. Since the conventional methods are far from providing required high efficiency, they will not be focused on this section. However, further readings can be proposed on improved conventional MPPT controllers (Çelik et al., 2018; Godoy et al., 2017; Jiang et al., 2012; Kasa et al., 2005; Petreuş et al., 2013).

4.2. Soft computing based MPPT algorithms

The recent development of microprocessors and decreased cost of microelectronics have facilitated the use of soft computing methods to comprise embedded powerful controllers. The nonlinear power characteristics of PV modules are also handled with soft computing methods which are derived from FLC, ANN and various evolutional algorithms. The most important contribution of soft computing based MPPT methods are their overcome capability on uncertainty, imprecision and low efficiency under extreme fluctuations that are mostly met in conventional MPPT algorithms (Salam et al., 2013). Nabipour et al. proposed a new MPPT method based on fuzzy approach after surveying the conventional methods and detecting the deficiencies in Nabipour et al. (2017). The FLC and ANN based algorithms are the most widely known and most flexible soft computing methods that are applied to improve existing MPPT approaches in several studies (Bendib et al., 2015; Karami et al., 2017; Messalti et al., 2017; Yilmaz et al., 2018).

The soft computing methods that are used to improve novel MPPT algorithms are listed by Salam et al. as shown in Fig. 17. In addition to FLC and ANN, evolutionary algorithms such as GA, differential evolution, ant colony optimization, and particle swarm optimization are presented in the literature. On the other hand, there can be found hybrid algorithms that are comprised by combining two or more soft computing methods such as ANN with FLC, ANN with PSO, GA with conventional methods and ANN with conventional methods (Salam et al., 2013). Since detailed surveys and comparisons on soft computing MPPT methods can be seen in several sources such as (Bendib et al., 2015; Bizon, 2016; de Brito et al., 2013; Eltawil and Zhao, 2013; Jiang et al., 2017; Karami et al., 2017; Messalti et al., 2017; Yilmaz et al., 2018), the detailed presentation of this section is based on applications and recent advances in micro inverter controllers.

Joshi et al. expresses that ANN, FLC, and GA are the three most prominent soft computing methods that are used in MPPT applications. In addition to pure use of these methods, an intersection of any type is used to generate hybrid MPPT algorithms as ANN FLC, ANN GA, and GA FLC in order to benefit robustness of each soft computing method. The ANNs are based on statistical learning methods operated at

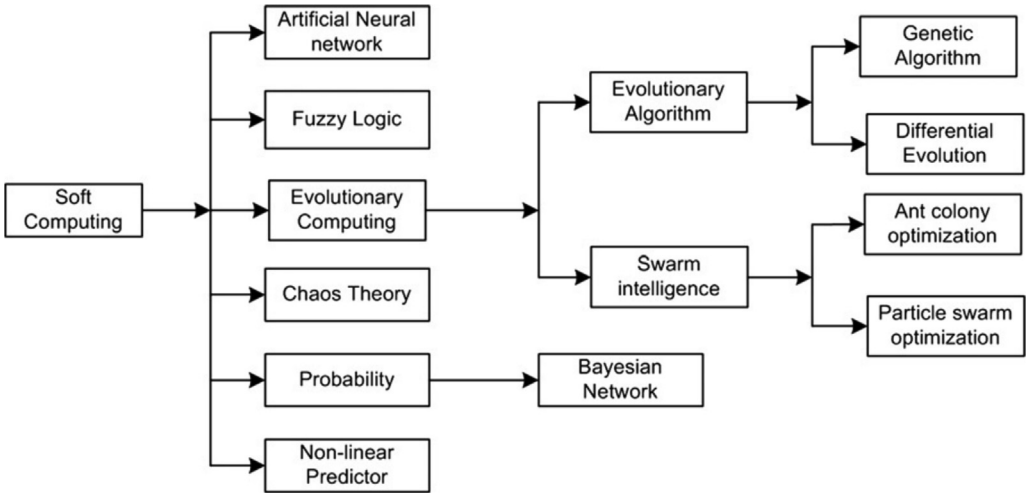

Fig. 17. Soft computing methods used to improve MPPT algorithms (Salam et al., 2013).

modelled biological neuron systems while FLCs are based on calculation of membership grades in a particular rule base, and GAs are improved by benefiting from biological systems and behaviours (Joshi and Arora, 2017). Most of the recent algorithms improved regarding to GA are known as evolutionary and swarm based algorithms such as particle swarm optimization (PSO) (Mohapatra et al., 2017; Zeddini et al., 2016), artificial bee colony (ABC) (Benyoucef et al., 2015; Fathy, 2015; Pilakkat and Kanthalakshmi, 2019), ant colony optimization (ACO), Cuckoo search, grey wolf optimization (GWO) and firefly algorithm (Bendib et al., 2015; Bizon, 2016; Jiang et al., 2017; Karami et al., 2017; Messalti et al., 2017; Yilmaz et al., 2018).

4.2.1. ANN based MPPT algorithms

A regular ANN system is comprised by many neurons which are used to determine the weighting rates of inputs, and the calculations in hidden layer to generate outputs. A featured ANN for MPP tracking requirements is seen in Fig. 18 where the input neurons are located at Layer h as solar insolation or irradiation, and temperature data. The Layer j accommodates the hidden layers and neurons determining the tracking capability of MPPT algorithm regarding the accuracy of weight calculation. Although there are different propagation methods as Levenberg-Marquardt, Back-Propagation, and Reinforcement Learning, most of the ANN designs are improved with back-propagation training algorithm due to its higher accuracy proven by increased hidden layer structure (Joshi and Arora, 2017; Salam et al., 2013).

A summary of ANN based MPPT algorithms has been tabularized in Table 5 where significant approaches and outcomes have been remarked. There are plenty of ANN based algorithms based on regular back-propagation methods while different researches based on other training and optimization methods. On the other hand, ANN based MPPTs have also been implemented to decrease power losses in DC-DC converter switching devices.

4.2.2. Evolutionary and swarm intelligence algorithms

The evolutionary algorithms such as GA and differential evolution or swarm intelligence based MPPT methods as ACO and PSO are being extensively researched due to their robust prediction and estimation capabilities (Joshi and Arora, 2017; Mohapatra et al., 2017; Salam et al., 2013).

The GA which is listed under evolutionary algorithms is a problem-solving method based on several biological evolution principles. The main target of a GA is to create better species comparing to their ancestors. Therefore, GA tries to find best solution by combining and random selection of existing genes. The GA algorithms are operated in the order of initialization, evaluation, genetic operations, and program termination. The initialization starts with referring to a set of solutions

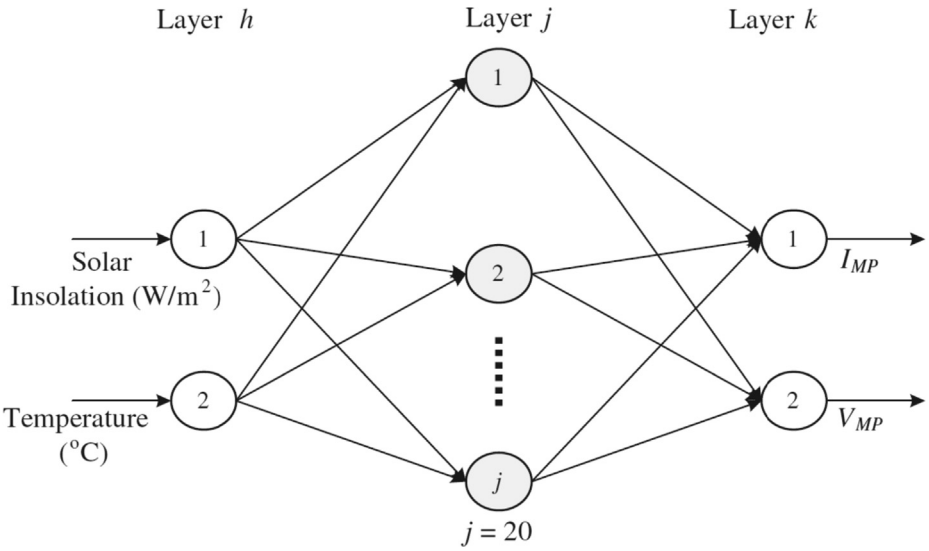

Fig. 18. Block diagram of an ANN based MPPT algorithm (Salam et al., 2013).

Table 5
Summary of ANN based MPPT applications.

Ref.	Converter	Control Inputs	ANN Type	Remarks
Boumaaraf et al. (2015)	Buck-boost	Open circuit voltage V_{OC} Short circuit current I_{SC}, Irradiation, Temperature	Back-Propagation	The ANN MPPT is improved to control buck-boost converter which interfaces a three-level NPC inverter. The accuracy of MPPT is compared to FLC MPPT where ANN based MPPT responded more rapid
Çelik and Teke (2017)	Interleaved Boost	Irradiation, Temperature	Levenberg-Marquardt	A hybrid MPPT method consisting of two loops where first one is ANN based reference point setting loop and second is P&O based fine tuning loop has been proposed. The controller provides 98.26% efficiency
Mekki et al. (2016)	N/A	Irradiation, Temperature	Levenberg–Marquardt, Variousback-propagation (resilient, Bayesian, Conjugate gradient, Gradient descent)	An ANN model operated with different propagation methods has been improved for estimating the output parameters of the PV module. The highest correlation of training set has been achieved with resilient back-propagation method
Kassem (2012)	Buck-boost	Irradiation	NARMA Multilayer Perceptron	A multilayer NN has been proposed in this study for buck-boost converter of PV array. The measurements and efficiencies have been compared to auto-tuning PID that lacks in efficiency
Rezk and Hasaneen (2015)	Boost	Irradiation, Temperature	Back-Propagation	ANN based MPPT has been proposed for triple-junction PV module. The converter efficiency compared in ANN and P&O MPPT operations
Harrag and Messalti (2019)	Boost	PV Voltage and Current	Neuro-Fuzzy	A neuro-fuzzy MPPT which is improved regarding to incremental conductance MPPT has been proposed
Saravanan and Ramesh Babu (2016)	SEPIC	PV Voltage and Current	Radial Basis Function Network (RBFN)	RBFN based ANN MPPT has been improved and compared to P&O and Incremental conductance MPPT algorithms. Switching power losses has been significantly decreased by ANN MPPT
Rizzo and Scelba (2015)	Full bridge	PV Voltage and Current (multiple inputs up to 8 couples)	Levenberg-Marquardt Back-Propagation	A global MPPT algorithms has been proposed under partial shading conditions. Multiple input ANN has been implemented with 8 couples of input parameters

provided by known chromosomes which are represented with a fixed code length. A fitness function is operated to evaluate each chromosome sets and a fitness value is defined for each chromosome. The genetic operators as selection, crossover, and mutation are generated by the fitness function for optimizing the population. The selection operation is applied to a certain population for comprising a mating base where crossover operators will be applied generating better genes by using code sets. The string matching is performed randomly and mutation operators start to be changing between 0 and 1 in an iteration. The random valued iteration is sustained to operate until the stop criterion achieved (Hadji et al., 2015; Harrag and Messalti, 2015; Kulaksız and Akkaya, 2012; Salam et al., 2013).

Besides GA, the differential evolution (DE) which has been proposed by Storn and Price is one of the most widely used evolutionary algorithm. It has attracted a significant interest as a global optimization algorithm due to its efficiency and simplicity. It is also based on similar operation orders as GA which starts with defining a population of n particle to obtain the optimal or best solution. The initial population is defined with random genes and then selection, crossover, and mutation loops are operated to modify and optimize the population. The best particles are selected and then mutation and crossover processes are repeated with a trial vector du_i for each target vector (Zaki Diab and Rezk, 2017). Tajuddin et al. (Tajuddin et al., 2013) define this D-dimensional parameter vector as $\boldsymbol{X} = (x_1, x_2, \ldots, x_D) \in R^D$ where $\boldsymbol{X}$ is the optimization criterion named objective function. The generated parameter vector is defined as follows,

$$\mathbf{X}^*: f(X) = min\, f(X) \tag{4}$$

where the feasible solution space is restricted between lower and higher design considerations as shown in (5),

$$L \leqslant X \leqslant H : L,\ H \in R^D \tag{5}$$

In a PV converter control, the DE is used to determine the best duty cycle D_{best} by benefiting from mutation factor and duty cycles which denotes the solution space as $[d_{min}, d_{max}]$. The mutation process is presented as follows to determine the donor vector or generated mutant particles;

$$dv_i = D_{best} + F{\cdot}(d_{r1} - d_{r2}) \tag{6}$$

where r_1 and r_2 are the mutual random integers, and F is the scaling factor. After the mutation stage, the crossover and selection operations are get started to determine the best particles (Salam et al., 2013; Tajuddin et al., 2013; Zaki Diab and Rezk, 2017). The block diagram of a DE based MPPT tracker is given in Fig. 19a where the searching mechanism have been shown in iterations (Zaki Diab and Rezk, 2017).

Although the PSO algorithm is listed under evolutionary computing algorithms, it differs from evolutionary algorithms since it is implemented regarding to cooperation and social behaviour determinations which is defined as swarm intelligence. PSO is based on a population as in other evolutionary algorithms where each particle provides an optimized and best solution to the problem. Each particle has a depended velocity that is determined by the update equation in search space. The equation is configured considering the recent experiences of each particle and collective behaviours. The fundamental approach is based on the idea that each particle has a certain velocity for displacement and to find the best solution. At the initial stage, random variables are located in search space and a cost function is produced to evaluate them. Afterwards, all particles update their positions in the direction of the particle which provides the best solution with the defined velocity. The update function is operated regarding to three parameters which are velocity of previous iteration, the particle best solution (p_{best}), and the global best solution (g_{best}). The first velocity equation is presented by Eberhart and Kennedy as follows;

$$V_i(t+1) = V_i(t) + c_1 R_1 \otimes \ (P_{best\_i} - X_i(t)) + c_2 R_2 \otimes (G_{best} - X_i(t)) \tag{7}$$

where t denotes the iteration number, i is the number of particle, the

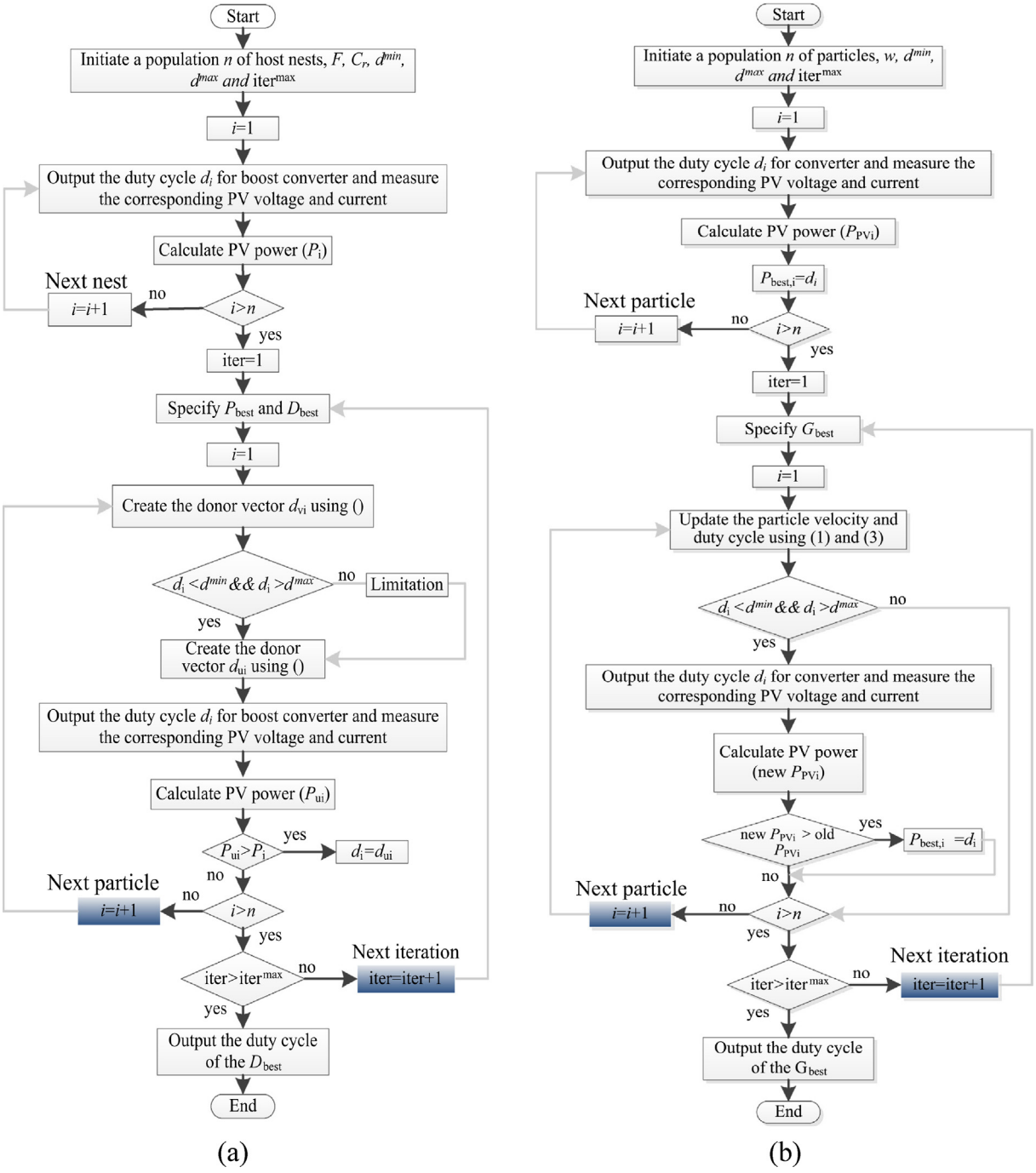

Fig. 19. Flowchart of evolutionary algorithms based MPPT, (a) DE, (b) PSO (Zaki Diab and Rezk, 2017).

vector P_{best_i} is the best solution of particle i at the certain point, the vector G_{best} denotes the best solution of all particles at the certain point while the c_1 and c_2 coefficients are the acceleration parameters, the vectors R_1 and R_2 are random numbers uniformly distributed between 0 and 1, and the symbol ⊗ represents element-by-element vector multiplication (Fermeiro et al., 2017). Rezk et al. proposed a PSO based MPPT algorithm regarding to (7) which is represented by the following equation (Rezk et al., 2017);

$$d_i^{k+1} = d_i^k + v_i^{k+1} \tag{8}$$

where v_i^{k+1} represents the step size at the iteration k + 1 which is depended to inertial weight ω, acceleration coefficients c_1 and c_2, and random values R_1 and R_2 between [0,1] (Fermeiro et al., 2017; Rezk et al., 2017);

$$v_i^{k+1} = \omega v_i^k + c_1 R_1 (P_{best} - d_i^k) + c_2 R_2 (G_{best} - d_i^k) \tag{9}$$

Fig. 19b represents the flowchart of a PSO based MPPT algorithm which is proposed by Zaki Diab and Rezk (2017). The comparison of DE and PSO algorithms provides several similarities in terms of operation steps comprised by initialization, updating and optimization to obtain best mutant or particle among others in the random search space. The first generated samples are applied to power converter for determining error rate of MPP, and then optimization is get started to achieve the best solution in both algorithms.

Table 6 represents a summary of evolutionary and swarm intelligence based MPPT algorithms that have been selected due to their differentiating features from literature survey. The conducted survey has shown that the swarm intelligence, and particularly PSO based

Table 6
Summary of evolutionary and swarm intelligence based MPPT applications.

Algorithm Type	Ref.	Control Inputs	Converter and Controller	Remarks
Genetic Algorithm	Harrag and Messalti (2015)	PV power	Boost Converter, Matlab Simulink	GA based P&O and PID controlled GA MPPT algorithms have been proposed as offline and online methods, and comparisons presented in terms of dynamic response, overshoot, and ripple reduction where GA based P&O overcomes
	Kulaksız and Akkaya (2012)	Irradiation, Temperature, and PV voltage	Three-phase full bridge inverter, PSIM Simulation	GA based ANN optimization has been proposed for MPPT control. The presented control method was promised to eliminate DC-DC converter requirement which enables to direct connection of PV to inverter
	Daraban et al. (2014)	PV voltage and current	Buck converter, DSP based control	GA based P&O algorithms has been proposed to improve efficiency under partial shading. The global MPPT control has been analysed with experimental testbed
	Lasheen et al. (2016)	PV voltage and current	Boost converter, PSIM Simulation	GA based constant voltage (CV) MPPT has been proposed for increasing the tracking efficiency
Differential Evolution	Zaki Diab and Rezk (2017)	PV voltage and current	Boost Converter, Matlab Simulink	Flower pollination and differential evolution algorithms have been proposed to decrease partial shading effect in building integrated PV systems
	Tajuddin et al. (2013)	PV voltage and current	Buck-boost converter, PLECS Simulation	A DE based MPPT has been proposed to analyse the performance comparing to hill climbing MPPT in terms of the dynamic response under rapid and large irradiation fluctuations. The performance of DE verified by authors
	Ramli et al. (2015)	PV voltage and current	Buck-boost converter, PV solar array simulator based experimental system	A new MPPT approach has been proposed named modified DE to overcome random selection drawbacks of regular DE MPPT. The results have been compared and evaluated under partial shading conditions
	Xiong et al. (2018)	PV voltage and current	N/A, experimental	An improved DE MPPT algorithm has been proposed with the name of whale optimization algorithm and compared to conventional DE MPPT in terms of different irradiation, temperature, and weather conditions
	Zhao et al. (2018)	PV voltage and current	SGSADE and CEC2017 benchmark	A novel hybrid algorithm based on self-adaptive Gravitational Search Algorithm (GSA) and DE is proposed for solving single objective optimization. The self-adaptive mechanism has been proposed
	Muhsen et al. (2019)	Weather data and component specifications	N/A, simulation	A decision making system has been improved to determine optimal sizing for a standalone PV system. The algorithm has been improved with multi-objective DE methods
Swarm Intelligence Based Algorithms (ACO, PSO, Cuckoo)	Fermeiro et al. (2017)	PV voltage and current	Boost converter, TMS320F28027 DSP	The conventional PSO algorithm has been improved to obtain more robust control in global and local best particles
	Rezk et al. (2017)	PV voltage and current	Boost Converter, Matlab Simulink	PSO and Cuckoo Search (CS) MPPT algorithms have been proposed and compared to incremental resistance MPPT
	Titri et al. (2017)	PV voltage and current	Boost Converter, Matlab Simulink	ACO MPPT has been improved and compared to conventional and soft computing methods such as P&O, ANN, FLC, ANFIS, FL GA, and PSO based MPPT algorithms
	Mosaad et al. (2019)	Irradiation, Temperature	Boost Converter, Matlab Simulink	CS based MPPT has been proposed and compared to ANN and P&O MPPT methods
	Sundareswaran et al. (2015)	PV voltage and current	Boost Converter, Simulation and PIC microcontroller	A new PSO method has been proposed and compared to regular PSO and P&O MPPT algorithms for evaluating the efficiency under partially shading conditions
	Oshaba et al. (2015)	Irradiation, Temperature	Buck-boost Converter, Matlab Simulink	Bat search algorithm has been proposed as an alternative to PSO MPPT and the improved method has been compared for a motor drive application which was supplied by PV
	Yang et al. (2019)	Irradiation, Temperature	Boost converter, DS1104 HIL experimental setup	A novel evolutionary algorithm named memetic salp swarm algorithm (MSSA) has been proposed. The proposed MPPT compared to INC, GA, PSO, ABC, CS, grey wolf optimizer (GWO), SSA, and teaching-learning-based optimization (TLBO) MPPTs
	Mirza et al. (2019)	PV voltage and current	Boost Converter, Matlab Simulink	Adaptive Cuckoo Search Optimization (ACO), General Regression Neural Network GRNN), Fruit fly Optimization (FFO), and Dragonfly Optimization (DFO) MPPT algorithms proposed
	Douiri (2019)	Irradiation, Temperature, output voltage	SEPIC converter, Simulink,	PSO optimized neuro-fuzzy MPPT improved and dynamic response of algorithms compared to existing models
	Saad et al. (2018)	PV voltage and current	Boost Converter, Matlab	Improved PSO MPPT presented for dynamic response and steady-state performance analysis of DC microgrid
	Dileep and Singh (2017)	PV voltage and current	SEPIC Converter, OPAL-RT OP5060	Adaptive PSO MPPT has been proposed to improve overall efficiency for GMPP tracking

algorithms are comprising most of the soft computing MPPT methods. The surveyed and summarized studies in Table 6 show that an increasing interest exist on swarm intelligence-based algorithms for improving competitive MPPT methods. The recently proposed researches present more efficient outcomes comparing to conventional PSO based MPPTs in terms of adaption to partial shading and rapidly changing weather conditions. On the other hand, the meta-heuristic methods have been proposed mimicking the behaviours of many different swarms such as bats, wolves, cuckoos, fireflies, and others in addition to ant or artificial bee colonies.

5. Device topologies in inverter section

Despite their low power application capabilities, the string and micro inverters are being paid increasing attention in grid-connection of PV systems and modules. The achieved technological improvements and decreasing costs of power electronics and device developments have leveraged opportunities on use of single-phase inverters. The galvanic isolation is one of the most widely discussed title in circuit topologies since the HF transformer increases the cost but provides no special solution for isolation. However, the capacitive isolation enables designers to build transformerless topologies with additional cares on safety requirements (Siwakoti and Blaabjerg, 2018). If we recall the inverter topologies given in figures Fig. 4, Fig. 7 and Figs. 9–14, it can be seen that the grid connections are performed by commonly using H4, and novel topologies such as H5, oH5, H6 and HERIC type inverter section that follows the HF transformer or output of intermediate DC-link stage.

Hasan et al. have presented a few additional inverter topologies in a review (Hasan et al., 2017) where most of them are based on flyback converter stage that is followed by center-tapped HF transformer and a full bridge converter as shown in Fig. 20. Sukesh et al. proposed a micro inverter topology by using proven cost-effective flyback converter in Fig. 20a (Sukesh et al., 2014). The proposed converter has been operated in BCM mode since the power transfer capability of flyback converter is limited in DCM operation. The primary side MOSFET S_m is switched on for charging the magnetizing inductance L_m to achieve reference current value. The charged current generates the required energy storage which will be transferred to utility grid by switching S_{p1} and S_{n1} devices regarding to positive and negative half-cycles of grid voltage (Sukesh et al., 2014).

The proposed topology ensures reliable operation due to BCM mode and switching controls. An alternative topology shown in Fig. 20b is titled flyback MIC which has drawn significant attention in recent years inverter, and proposed as interleaved flyback MIC (IFMIC) in Edwin et al. (2014). The main contributions of IFMIC are noted as equal load sharing on dc converter stage, reduced input voltage and pseudo-DC link voltage ripples, and reducing the EMI noise by current sharing. The solar inverter is operated in CCM mode at interleaved flyback stage, and fourth-order LC filter has been implemented to attenuate distortions before transferring the converted power to utility grid.

The inverter stages of Fig. 20b and c are operated at line-frequency since they have been implemented with gate turn off (GTO) switches. Although the topology is based on fundamental H4 inverter, GTO based architecture eliminates LF transformer requirement on secondary side of HF transformer due to decreased voltage stress because of GTO switches. Since the primary side converter is comprised by interleaved flyback, the BCM operation mode is the most appropriate method for increasing the transferred power rate in such topologies.

The primary current of HF transformer is forced to track reference

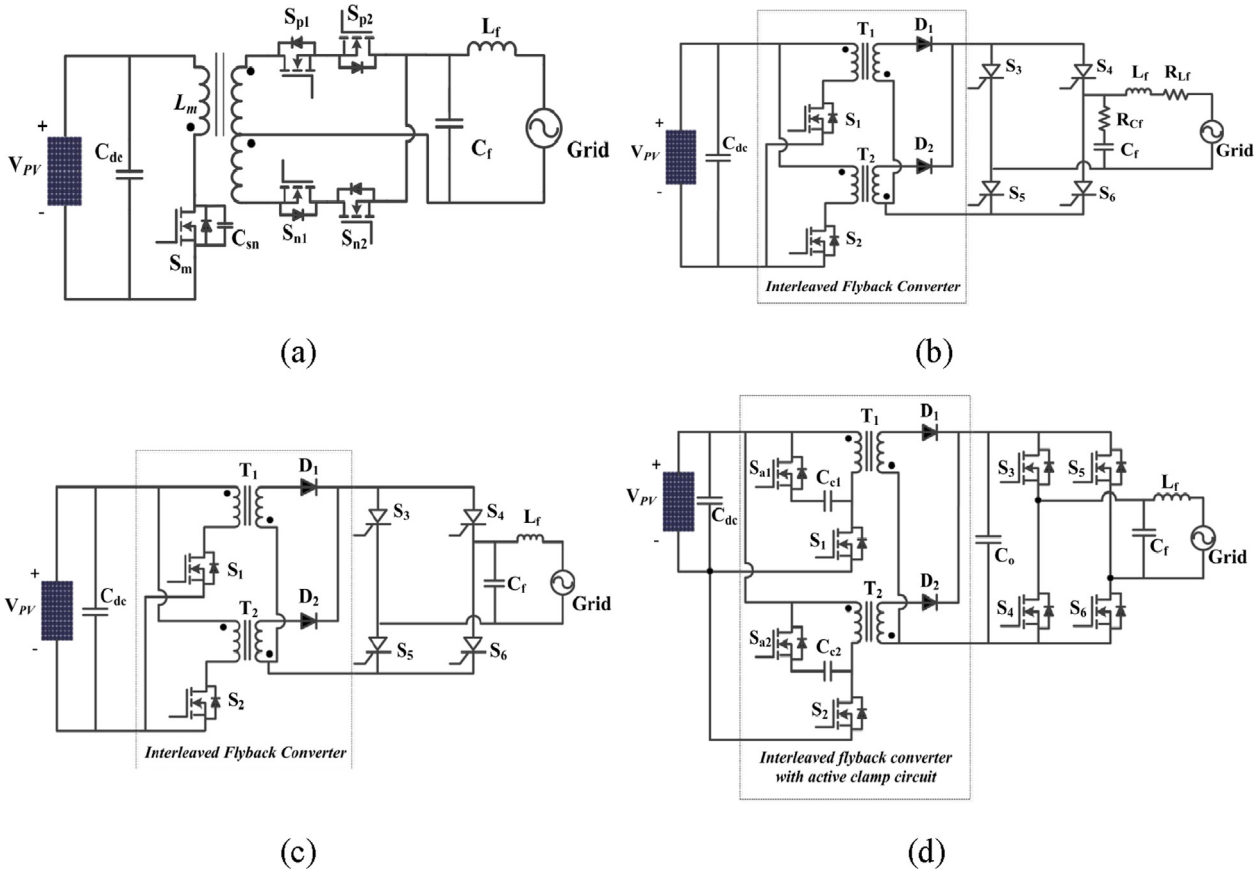

Fig. 20. Various alternative inverter topologies used in solar inverters (Hasan et al., 2017), (a) Single flyback inverter with soft switching (Sukesh et al., 2014), (b) CCM control interleaved flyback inverter (Edwin et al., 2014), (c) BCM control interleaved flyback inverter (Gao et al., 2014), (d) ILFI with soft switching (Kim et al., 2013).

Table 7
Comparison of recent inverter stage topologies in solar micro inverters.

Ref.	Component Numbers				Active switch number at each half-cycle		Switching Method	Peak Efficiency	Galvanic Isolation
	S	D	C	L	(+)	(−)			
(Islam et al., 2015) Flying Capacitor	4	1	2	0	2	2	Hard switching	99.2%	No
(Xiao et al., 2011) oH5	6	0	2	0	3	3	Active Clamping	97.2%	No
(Kerekes et al., 2011) H4-ZVR	5	5	2	0	2	2	Hard switching	94.88%0	No
(L. Zhang et al., 2014) H5	5	0	2	2	3	3	Hard switching	96.78%	No
(L. Zhang et al., 2014) H6	6	0	2	2	3	2	Hard switching	97.09%	No
(L. Zhang et al., 2014) HERIC	6	0	2	2	2	2	Hard switching	97%	No
(Sukesh et al., 2014) Flyback Inverter	5	0	2	1	2	2	BCM soft switching	94%	Yes
(Edwin et al., 2014) ILF Inverter	6	2	2	1	2	2	CCM soft switching	95.7%	Yes
(Kim et al., 2013) ILF Inverter	8	2	5	1	2	2	DCM soft switching	95.11%	Yes
(Gao et al., 2014) ILF Inverter	6	2	2	1	2	2	BCM soft switching	94%	Yes
(Vinnikov et al., 2019) Optiverter	9	2	6	5	4	4	Quasi-resonant soft switching	95.3%	Yes
(H. Wang et al., 2018) Aalborg Inverter	6	6	1	1	3	2	CCM	NA	Yes
(Liu et al., 2017) Modified LLCL Aalborg Inverter	6	4	2	4	3	3	Soft switching	98.3%	No

S = Switch, D = Diode, C = Capacitor, L = Inductor, (+) = positive half-cycle, (−) = negative half-cycle.

Table 8
Grid connection standards for micro inverters (Hasan et al., 2017; DeBlasio, 2009; International Electrotechnical Commission and Oruganti, 2014; Meneses et al., 2013).

Requirement	IEC 61727		IEEE 1547-2008		EN61000-3-2		VDE	
Nominal Power	10 kW		30 kW		16A 230 V		–	
	Order (h)	Limit	Order (h)	Limit	Order (h)	Limit (A)	Order (h)	Limit (A/MVA)
Harmonic Content	3–9	4.0%	3–9	4.0%	3	2.31	3	3
	11–15	2.0%	11–15	2.0%	5	1.14	5	1.5
	17–21	1.5%	17–21	1.5%	7	0.77	7	1
	23–33	0.6%	23–33	0.6%	9	0.4	9	0.7
			> 35	0.3%	11	0.33	11	0.5
					13	0.21	13	0.4
	Even harmonics are limited to 25% of the odd harmonic limits				(15–39)	2.25/h	17	0.3
							19	0.25
					2	1.08	23	0.2
					4	0.43	25	0.15
					6	0.3	25–40	3.75/h
	THD < 5%				(8–40)	1.84/h	Even	1.5/h
							greater than40	4.5/h
DC Current Injection	< 1% of rated output current		< 0.5% of rated output current		< 0.22A		< 1A, max. trip time = 0.2 s	
Voltage Deviations	Range (%)	Time (s)	Range (%)	Time (s)	Range (%)	Time (s)	Range (%)	Time (s)
	V < 50	0.1	V < 50	0.16	–		V < 85	0.2
	50 ≤ V < 88	2	50 ≤ V < 88	2			V ≥ 110	0.2
	110 ≤ V < 120	2	110 ≤ V < 120	1				
	V ≥ 120	0.05	V ≥ 120	0.16				
Frequency Deviation	Range (Hz)	Time (s)	Range (Hz)	Time (s)	Range (Hz)	Time (s)	Range (Hz)	Time (s)
	49 < f < 51	0.2	59.3 < f < 60.5	0.16			47.5 < f < 50.2	0.2

current, and magnetizing is maximized (Gao et al., 2014). Another IFMIC topology which has been named as interleaved flyback inverter (ILFI) has been proposed by Kim et al. as seen in Fig. 20d (Kim et al., 2013). The topology uses a decoupling capacitor for eliminating double-frequency harmonics at 120-Hz of 60 Hz line frequency. Besides the converting unfolding inverter switches to IGBTs, this inverter structure has been proposed with a novel control method based on single MPPT for both interleaved phases and PLL for inverter stage (Kim et al., 2013). A detailed comparison of recent device topologies used in inverter stage of micro inverters has been summarized in Table 7 where several particular features such as component numbers, active switch numbers at each half-cycle, switching method, peak efficiency, and galvanic isolation have been listed. The flying capacitor topology presented in Islam et al. (2015) provides the highest efficiency with the least component number. On the other hand, it should be noted that the transformerless topologies are reported to provide higher efficiency than isolated architectures. Another noticeable issue from Table 7 is on ILF topologies. Although these topologies are paid more attention in recent architectures, the peak efficiencies given in Edwin et al. (2014), Gao et al. (2014), Kim et al. (2013), Sukesh et al. (2014) are lower almost than all others.

The efficiency and reliability of inverter stage are mostly ensured by control method in power transfer operation of micro inverter to utility grid. Therefore, the control methods and controllers implemented for grid connection are comprehensively introduced and discussed in the following section.

6. Inverter controllers

Since the solar inverters are responsible for connecting the generated power at PV side to utility grid, two separate control infrastructures are required where the first one is located at PV side while the other one is operated at the output of inverter to interface the entire device with utility grid. The PV side control represents converter side

control mechanism which is mostly MPPT as discussed earlier. On the other hand, grid side control is requested to improve power quality and efficiency of inverter to ensure reliable operation. Therefore, grid side controller of solar inverter should meet grid interconnection requirements, provide secure grounding, and power decoupling features. The inverters improved for operating in single-phase grids should comply with grid requirements described by several international and regional standards. The control architectures of inverters are classified into three categories due to device topology as two-stage, single stage without dc converter, and power control shifting phase (PCSP) approaches (Hassaine et al., 2014; Mahela and Shaik, 2017; Meneses et al., 2013). All three methods are improved to achieve fast dynamic response, instant current control, and simple device architecture while PCSP provides additional reactive power control opportunity.

A micro inverter operating in grid-connected mode should satisfy the grid connection standards in terms of power quality, THD ratios, islanding detection, grid interfacing limits for voltage and frequency, and grounding. Menenes et al. have presented a list of standard requirements in Meneses et al. (2013) which are shown in Table 8 that presents a summary of international standards which should be followed to ensure grid requirements in micro inverter interconnection to grid. The most important concerns are related to THD ratios, voltage and frequency deviations, and DC current injection ratios. The injection ratio of DC current is a serious indicator for transformerless device topologies and should be lower than 1% of rated output current of inverter. However, such a low current rate requires a robust and precise controller for the micro inverter. Although the transformerless topologies bring increased efficiency, light weight, and decreased cost, they eliminate the galvanic isolation which causes leakage ground currents with CMV deviations.

The grounding is another important issue in micro inverter controllers for decreasing the leakage ground currents. On the other hand, power demand is expected to be continuously met by a single PV module in micro inverter applications. Since a single PV module is capable to generate pure DC power at any operation instant, an internal energy storage mechanism which is titled as power decoupling and mostly supplied by a capacitor is required. The decoupling capacitor, which is either electrolytic or film type stores the generated energy and eliminates double line-frequency deviations. The power decoupling is also an important control procedure in micro inverter applications besides grid interconnection, grounding and power quality controls (Mahela and Shaik, 2017; Meneses et al., 2013).

Although it is easy to connect the three-phase inverters to utility grid by using regular PLL based controllers, the design of dc-bus voltage control scheme and current injection to grid are challenging issues in single-phase inverters due to double line-frequency ripples and non-trajectory nature of single-phase. Table 9 represents a list of single-phase inverter designs and proposed controllers for grid interconnection. The deadbeat control which is one of the widely known digital control schemes has been proposed by Mattavelli (2005) for single-phase uninterruptible power supply (UPS) application. The controller has been implemented by using output voltage and inductor current of inverter where a state estimator has been proposed to overcome computational delay. Castilla (2008) proposed a linear current control scheme for single-phase grid-connected PV inverters. In spite of regular harmonic compensators that are parallel connected to tracking regulator, the serial connected harmonic compensator has been proposed to improve synchronization accuracy and eliminating the PLL requirement in Castilla (2008). In another study, Miret et al. (2009) proposed a selective harmonic compensator to eliminate certain orders of voltage and current harmonics at the output of inverter. The controller focuses on generating a reference current to detect the most influential harmonic orders and forces modulator to attenuate the detected harmonics. A proportional resonant (PR) current feedback control method has been proposed in Shen et al. (2010) to achieve synchronization for a grid-connected single-phase inverter. The output stage of inverter has been comprised by an LCL filter where the weighted average of the inverter current and the grid current have been used as feedback parameters in controller. Ho et al. (2009) proposed a constant-frequency hysteresis current controller to overcome interconnection deficiencies while a rotating-sliding-line-based sliding mode controller (SMC) for single-phase UPS inverters has been presented in Komurcugil (2012). Besides these control methods, it is seen that active damping, droop, and repetitive control based schemes are widely used in grid connection of single-phase inverters (Bao et al., 2014; Eren et al., 2015; Guo et al., 2014; Xu et al., 2014; Yao and Xiao, 2013; Zhu et al., 2016).

Xu et al. have presented a summary of active damping based methods that are improved by using a single current feedback in Xu et al. (2014). Although the operation stability is guaranteed under certain current and filter parameters, it is not easy to ensure achieving a high bandwidth in operation. Therefore, a number of improvements have been done in general active damping controllers considering the LCL output filter is used in single-phase inverter as shown in Fig. 21 where filter is comprised by inverter-side inductor L_1, capacitor C_1, grid-side inductor L_2, equivalent parasitic resistors r_1 and r_2. The inverter output voltage is denoted with u_{inv} while the grid voltage is u_g and injected grid current i_g that is sampled for closed-loop current control.

The equation denoting the relation between grid voltage and injected grid current is represented in (10) while the natural resonance frequency that may cause to resonating current is seen in (11);

$$G_{u_{inv}}^{i_g} = \frac{1}{L_1L_2C_1s^3 + (r_2L_1 + r_1L_2)C_1s^2 + (L_1 + L_2 + r_1r_2C_1)s + r_1 + r_2} \tag{10}$$

Table 9
Single-phase inverter controllers and features.

Ref.	Topology and Rated Power	Application	Filter	Controller Type	Reference Parameter	Feedback Loop
Mattavelli (2005)	Full Bridge – *2 kVA*	UPS	LC	Deadbeat	V_O, I_{Inv}	Multiple
Castilla (2008)	Full Bridge – *1.5 kW*	PV	LCL	Current control	I_{Inv}, I_{Ref}	Single
Miret et al. (2009)	H4 – *500 VA*	APF	NA	Selective compensator	V_O, I_{Inv}	Multiple
Shen et al. (2010)	Two-stage (H4 converter, Half Bridge inverter – *5 kW*)	Fuel Cell	LCL	PR current control	Weigthed average of I_{Inv}, I_{Grid}	Single
Ho et al. (2009)	H4 – *300 W*	DG	L	Constant *f* hysteresis *I*	I_L, V_{Grid}	Single
Komurcugil (2012)	H4 – *NA*	UPS	LC	Sliding mode control	V_O, I_O	Multiple
Yao and Xiao (2013)	Dual-Buck Full-Bridge – *1 kW*	VSI	LC	Hysteresis *I*	I_{Grid}, V_{Grid}	Multiple
Guo et al. (2014)	H4 – *NA*	VSI	L	Repetitive	I_{Grid}	Single
Xiao et al. (2011), Xu et al. (2014)	oH5 – *5 kW*	PV	LCL	Active damping (AD) based	I_{Grid}, V_{Grid}	Multiple
Bao et al. (2014)	H4 – *5 kW*	VSI	LCL	Capacitor current AD	I_{Grid}, V_{Grid}	Multiple
Eren et al. (2015)	H4 – *1.8 kW*	PV, Wind	LCL	Droop control	V_{Bus}, I_{Grid}	Multiple
Zhu et al. (2016)	H4 – *NA*	VSI	LCL	Fractional-order repetitive control	I_{Grid}	Single

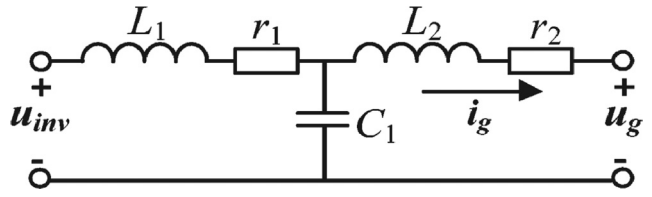

Fig. 21. LCL filter of grid-connected single-phase inverter (Xu et al., 2014).

$$f_{res} = \frac{1}{2\pi}\sqrt{\frac{L_1 + L_2}{L_1 L_2 C_1}} \tag{11}$$

Fig. 22 represents improved active damping control methods that are developed by using the single-phase grid current control method. The controller using grid current injection method is seen with black lines in Fig. 22 where k_g is the grid voltage, i_{ref} is the reference current, and $G_c(s)$ denotes the current regulator which is followed by LCL filter blocks. The controller seen in Fig. 22a is improved with active damping method based on capacitor current control loop that is controlled by k_{AD} proportional feedback parameter. The transfer function of this closed-loop controller denoting the injected current is proposed as seen in (12) that is achieved by revising (10);

$$G_{i_{ref}}^{i_g} = \frac{G_C(s)}{L_1 L_2 C_1 s^3 + k_{AD} L_2 C_1 s^2 + (L_1 + L_2)s + G_C(s)} \tag{12}$$

The transfer function of u_g to i_g is presented in this situation as follows;

$$G_{u_g}^{i_g} = \frac{-k_{AD} C_1 s - L_1 C_1 s^2}{L_1 L_2 C_1 s^3 + k_{AD} L_2 C_1 s^2 + (L_1 + L_2)s + G_C(s)} \tag{13}$$

Since there is a correlation exist between capacitor current and injected grid current, the capacitor current feedback is inserted to developed controllers seen in Fig. 22b–d. On the other hand, an additional closed-loop proportional controller which is based on grid-side inductor voltage is added to active damping controllers seen in Fig. 22c and d for decreasing the current harmonics. The revised transfer function of u_g to i_g is obtained as seen in (14);

$$G_{u_g}^{i_g} = \frac{-L_1 C_1 s^2}{L_1 L_2 C_1 s^3 + k_{AD} L_2 C_1 s^2 + (L_1 + L_2)s + G_C(s)} \tag{14}$$

It is seen that the first-order derivative parameter is removed from numerator, and a second-order derivative feedback ($k_{AD}L_2C_1s^2$) denoting the injected grid current exist to reject the resonance (Xu et al., 2014).

Although the active damping control schemes presented in Xu et al. (2014) do not include PLL controller, Bao et al. have proposed a similar active damping based controller that uses capacitor–current as feedback parameter (Bao et al., 2014). The circuit schematic of single-phase grid-connected VSI with LCL filter is seen in Fig. 23a while the transfer function of multiple feedback controller is shown in Fig. 23b. In the proposed application of (Bao et al., 2014), authors express that PLL is used to synchronize the the reference of injected grid current i_g with the grid voltage v_g. The feedback coefficient and gain of injected currents are represented by H_{i1} and H_{i1} blocks respectively. The injected grid current regulator is described with $G_i(s)$ while the transfer function of inverter is denoted with G_{inv} block.

Zeb et al. have presented a list of inverter controllers as non-linear group including SMC, partial feedback linearization (PFL), hysteresis, H∞, model predictive (MPC), ANN, repetitive, FLC, and autonomous controllers in Zeb et al. (2018). However, the surveyed controllers and control schematics presented in Zeb et al. (2018) are mostly proposed for three-phase inverters and medium power applications. Therefore, the PLL based control algorithms are listed in three-phase applications.

7. Discussion and future studies

It is seen that an increasing and extensive interest has been paid to string and micro inverters that are improved mostly to be used in single-phase applications. The main motivation behind this situation is highly created by integration of distributed energy resources (DERs) to utility grid. Many countries are promoting the DG for individuals besides the industrial plants, and a wide variety of regulations are available for subsiding residential users that are now defined as prosumer. Therefore, the single-phase inverters are increasing their importance and widespread use in RES integration in microgrid and nanogrid architectures.

The reviewed studies and papers listed in current literature have shown that there are many aspects affecting the design and implementation of a single-phase inverter exist. Most of the leading factors are related to isolation requirement, single or two-stage architecture, MPPT control approaches, inverter stage topology, and inverter controllers in grid-connection. Although the isolation was an industry standard and a strict requirement until a few years ago, it is seen that the novel circuit topologies tackle the leakage current elimination by several capacitive isolation methods. On the other hand, the input

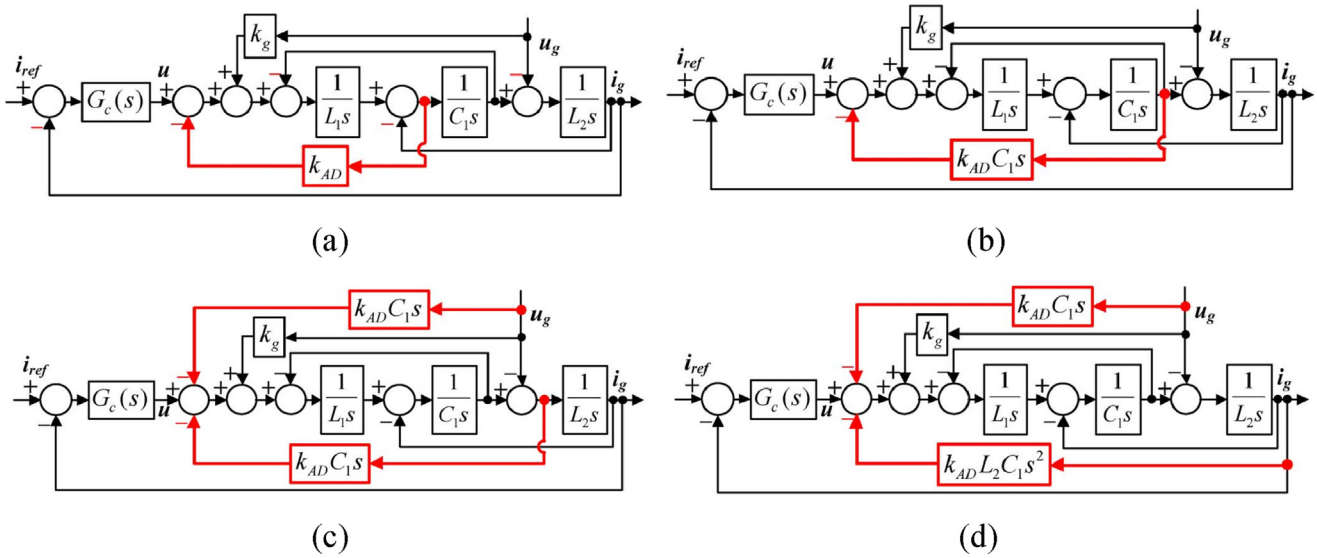

Fig. 22. Active damping based control schemes (Xu et al., 2014) (a) capacitor current feedback, (b) equivalent capacitor voltage feedback, (c) equivalent grid-side inductor voltage feedback, and (d) equivalent injected grid current feedback.

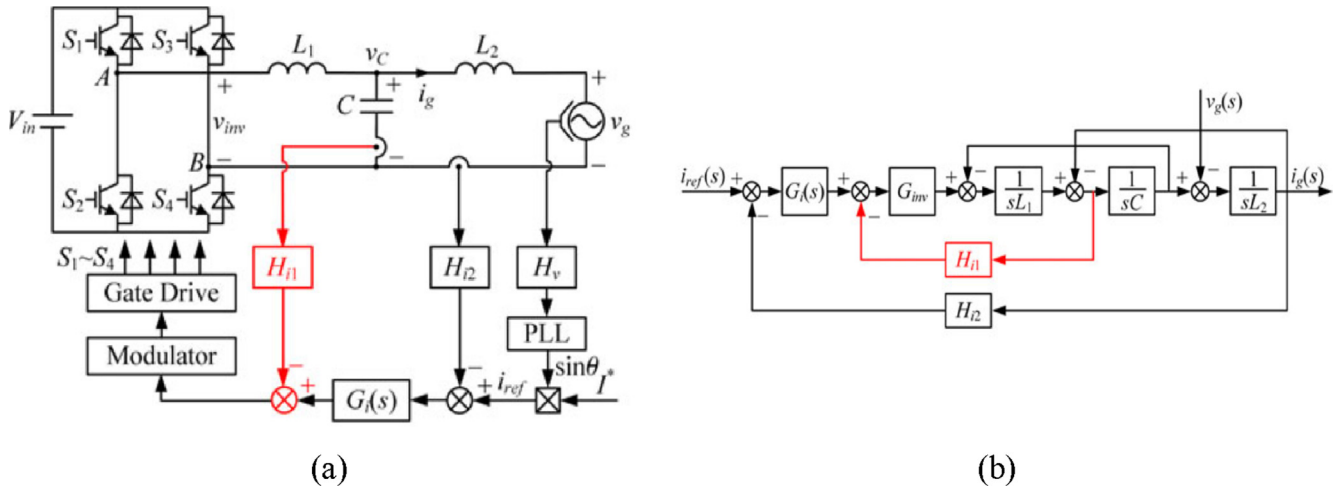

Fig. 23. PLL based active damping control scheme (Bao et al., 2014) (a) circuit schematic, (b) transfer function.

capacitor arrangements are also proposed to overcome leakage current and power decoupling requirements in literature. The multi-stage topologies are convenient to eliminate parasitic effects. Therefore, the reliability, power density, overall cost, and performance of transformerless inverter topologies are optimized in recent designs. The improved power semiconductors such as SiC and GaN based mosfets are replacing the conventional Si switching devices, and thus the efficiency of inverter is significantly increased by decreasing the switching and cooling losses. It is foreseen that increased availability of SiC and GaN devices will allow to replace IGBTs with MOSFETs in inverter topologies, and thus high frequency switching will be an industry standard. On the other hand, the operating mode of switching device in a DC-DC converter affects the efficiency of inverter where DCM or BCM modes are remarkable in addition to regular CCM.

It is also seen that the efficiency of DC-DC converter stages are improved by novel topologies such as flyback, interleaved flyback, and resonant topologies while the soft switching methods based MPPT controllers are promising higher efficiency even under partial shading operations in PV applications. The conventional MPPT methods such as P&O, InCon, and Hill-climbing are given up while the increased interest has been directed to ANN based, evolutionary and swarm intelligence algorithms. The surveyed papers have shown that evolutionary and swarm intelligence based MPPT algorithms provide higher efficiency in local and global MPPT processes. Therefore, it should be noted that regular and conventional MPPT methods will not be considered any longer.

Another remark achieved from literature surveys is the circuit topologies in inverter section of a single-phase solar inverter that are beyond the conventional H-bridge, namely H4, or two-level topologies. The most widely used innovative topologies are improved with H5, oH5, H6, H6D1, H6D2, HERIC, and resonant circuit architectures. It is anticipated that novel inverter topologies will be improved to overcome reliability, voltage stress on switches, current injection control, and transformerless operation issues. Moreover, it is obvious that the improvements seen in circuit topologies will also require novel control methods and schemes. The PLL based control methods were industry standard in grid-connection of three-phase inverters, and they have been adapted to single-phase interconnection. However, there are many reliability issues and challenging situations have been reported for single-phase PLL applications in the literature. The literature review have also shown that many novel interconnection methods have been proposed without PLL in single-phase applications. The active damping, hysteresis band controllers, selective harmonic elimination compensator, and PR controller are some of these controllers. It is anticipated several alternative control methods replacing the PLL requirement will be proposed for interconnection of PV inverters to single-phase grid.

As a summary of discussions, the multi-stage single-phase PV inverters are required to be improved in terms of power decoupling, efficiency under partial shading, operation mode control of converter stage, grid-connection and islanding detection of unfolding stage, and device topologies to eliminate potential hazards of transformerless operation.

8. Conclusion

The integration of PV power plants to utility grid has been rapidly increased in single-phase applications due to microgrid and nanogrid concepts that are brought by DG. Such a widespread application area which is integrated to utility grid should be managed in accurate, efficient, and reliable ways. There are numerous standards defining the interconnection and disconnection of single-phase inverters to utility grid available. The solar inverters are one of the most extensively researched topics in emerging power electronics due to their variety in circuit and control architectures. In this paper, a comprehensive literature review has been presented considering string and micro inverters which differentiate from central inverter in terms of power level and application areas. The targeted survey group has been comprised by single-phase grid-connected inverters, and single and multi-stage inverters have been reviewed. The multi-stage topologies that are implemented with DC-DC converter and unfolding inverter stages have been researched for novel circuit topologies and recent control methods. The widely known and conventional topologies have been disregarded to provide further focus on emerging systems. The literature survey has shown that there is an increasing tendency on isolated and resonant DC-DC converter topologies due to galvanic isolation requirements. However, non-isolated topologies have also been researched in order to eliminate HF transformer requirement and for removing the leakage current by capacitive coupling. It has also been noted that the unfolding stage topologies improved by using novel structures differing from conventional two-level and H-bridge circuit schemes. In addition to circuit architectures, the control methods of converter and unfolding stages have also been surveyed where novel MPPT methods, and grid-connection schemes have been presented in a comprehensive way. The literature surveys have been enriched with figures illustrating device topologies and control methods, and tabularized summaries have been presented to provide further reading on certain issues. As a final remark, this review is anticipated to be a comprehensive source for researchers and professionals who are investigating solar string and micro inverter in terms of device topologies, control methods, development and implementation directions.

Declaration of Competing Interest

The authors declare that they have no known competing financial interests or personal relationships that could have appeared to influence the work reported in this paper.

References

Abdel-Rahman, S., 2012. Resonant LLC Converter: Operation and Design. Infineon Technologies North America (IFNA) Corp. 19.

Ahmad, Z., Singh, S.N., 2018. Improved modulation strategy for single phase grid connected transformerless PV inverter topologies with reactive power generation capability. Sol. Energy 163, 356–375. https://doi.org/10.1016/j.solener.2018.01.039.

Ahmad, Z., Singh, S.N., 2017a. Comparative analysis of single phase transformerless inverter topologies for grid connected PV system. Sol. Energy 149, 245–271. https://doi.org/10.1016/j.solener.2017.03.080.

Ahmad, Z., Singh, S.N., 2017b. An improved single phase transformerless inverter topology for grid connected PV system with reduce leakage current and reactive power capability. Sol. Energy 157, 133–146. https://doi.org/10.1016/j.solener.2017.08.007.

Ahmed, J., Salam, Z., 2017. An accurate method for MPPT to detect the partial shading occurrence in a PV system. IEEE Trans. Ind. Inform. 13, 2151–2161. https://doi.org/10.1109/TII.2017.2703079.

Ankit, Sahoo, S.K., Sukchai, S., Yanine, F.F., 2018. Review and comparative study of single-stage inverters for a PV system. Renew. Sustain. Energy Rev. 91, 962–986. https://doi.org/10.1016/j.rser.2018.04.063.

Baka, M., Manganiello, P., Soudris, D., Catthoor, F., 2019. A cost-benefit analysis for reconfigurable PV modules under shading. Sol. Energy 178, 69–78. https://doi.org/10.1016/j.solener.2018.11.063.

Bendib, B., Belmili, H., Krim, F., 2015. A survey of the most used MPPT methods: conventional and advanced algorithms applied for photovoltaic systems. Renew. Sustain. Energy Rev. 45, 637–648. https://doi.org/10.1016/j.rser.2015.02.009.

Benyoucef, A., Soufyane, Chouder, A., Kara, K., Silvestre, S., Sahed, O.A., 2015. Artificial bee colony based algorithm for maximum power point tracking (MPPT) for PV systems operating under partial shaded conditions. Appl. Soft Comput. 32, 38–48. https://doi.org/10.1016/j.asoc.2015.03.047.

Bizon, N., 2016. Global maximum power point tracking (GMPPT) of photovoltaic array using the extremum seeking control (ESC): a review and a new GMPPT ESC scheme. Renew. Sustain. Energy Rev. 57, 524–539. https://doi.org/10.1016/j.rser.2015.12.221.

Boumaaraf, H., Talha, A., Bouhali, O., 2015. A three-phase NPC grid-connected inverter for photovoltaic applications using neural network MPPT. Renew. Sustain. Energy Rev. 49, 1171–1179. https://doi.org/10.1016/j.rser.2015.04.066.

Castilla, M., 2008. Linear current control scheme with series resonant harmonic compensator for single-phase grid-connected photovoltaic inverters. IEEE Trans. Ind. Electron. 55, 2724–2733. https://doi.org/10.1109/TIE.2008.920585.

Çelik, Ö., Teke, A., 2017. A Hybrid MPPT method for grid connected photovoltaic systems under rapidly changing atmospheric conditions. Electr. Power Syst. Res. 152, 194–210. https://doi.org/10.1016/j.epsr.2017.07.011.

Çelik, Ö., Teke, A., Tan, A., 2018. Overview of micro-inverters as a challenging technology in photovoltaic applications. Renew. Sustain. Energy Rev. 82, 3191–3206. https://doi.org/10.1016/j.rser.2017.10.024.

Chen, B., Gu, B., Zhang, L., Zahid, Z.U., Lai, J.-S.J., Liao, Z., Hao, R., 2015. A high-efficiency MOSFET transformerless inverter for nonisolated microinverter applications. IEEE Trans. Power Electron. 30, 3610–3622. https://doi.org/10.1109/TPEL.2014.2339320.

Chen, K., Tian, S., Cheng, Y., Bai, L., 2014. An improved MPPT controller for photovoltaic system under partial shading condition. IEEE Trans. Sustain. Energy 5, 978–985. https://doi.org/10.1109/TSTE.2014.2315653.

Bao, Chenlei, Ruan, Xinbo, Wang, Xuehua, Li, Weiwei, Pan, Donghua, Weng, Kailei, 2014. Step-by-step controller design for LCL-type grid-connected inverter with capacitor–current-feedback active-damping. IEEE Trans. Power Electron. 29, 1239–1253. https://doi.org/10.1109/TPEL.2013.2262378.

Daraban, S., Petreus, D., Morel, C., 2014. A novel MPPT (maximum power point tracking) algorithm based on a modified genetic algorithm specialized on tracking the global maximum power point in photovoltaic systems affected by partial shading. Energy 74, 374–388. https://doi.org/10.1016/j.energy.2014.07.001.

de Brito, M.A.G., Galotto, L., Sampaio, L.P., e Melo, G.De.A., Canesin, C.A., 2013. Evaluation of the main MPPT techniques for photovoltaic applications. IEEE Trans. Ind. Electron. 60, 1156–1167. https://doi.org/10.1109/TIE.2012.2198036.

Díez-Mediavilla, M., Dieste-Velasco, M.I., Rodríguez-Amigo, M.C., García-Calderón, T., Alonso-Tristán, C., 2014. Performance of grid-tied PV facilities based on real data in Spain: Central inverter versus string system. Energy Convers. Manage. 86, 1128–1133. https://doi.org/10.1016/j.enconman.2014.06.087.

Dileep, G., Singh, S.N., 2017. An improved particle swarm optimization based maximum power point tracking algorithm for PV system operating under partial shading conditions. Sol. Energy 158, 1006–1015. https://doi.org/10.1016/j.solener.2017.10.027.

Dong, M., Tian, X., 2017. Dual-Mode interleaved flyback micro-inverter. In: 2017 Chinese Automation Congress (CAC). Presented at the 2017 Chinese Automation Congress (CAC). IEEE, Jinan, pp. 7719–7724. https://doi.org/10.1109/CAC.2017.8244175.

Douiri, M.R., 2019. Particle swarm optimized neuro-fuzzy system for photovoltaic power forecasting model. Sol. Energy 184, 91–104. https://doi.org/10.1016/j.solener.2019.03.098.

Dutta, S., Debnath, D., Chatterjee, K., 2018. A grid-connected single-phase transformerless inverter controlling two solar PV arrays operating under different atmospheric conditions. IEEE Trans. Ind. Electron. 65, 374–385. https://doi.org/10.1109/TIE.2017.2711577.

Edwin, F., Xiao, W., Khadkikar, V., 2012. Topology review of single phase grid-connected module integrated converters for PV applications. In: IECON 2012 - 38th Annual Conference on IEEE Industrial Electronics Society. Presented at the IECON 2012 - 38th Annual Conference of IEEE Industrial Electronics. IEEE, Montreal, QC, Canada, pp. 821–827. https://doi.org/10.1109/IECON.2012.6388645.

Edwin, F.F., Xiao, W., Khadkikar, V., 2014. Dynamic modeling and control of interleaved flyback module-integrated converter for PV power applications. IEEE Trans. Ind. Electron. 61, 1377–1388. https://doi.org/10.1109/TIE.2013.2258309.

Eltawil, M.A., Zhao, Z., 2013. MPPT techniques for photovoltaic applications. Renew. Sustain. Energy Rev. 25, 793–813. https://doi.org/10.1016/j.rser.2013.05.022.

Eren, S., Pahlevani, M., Bakhshai, A., Jain, P., 2015. An adaptive droop DC-bus voltage controller for a grid-connected voltage source inverter with LCL filter. IEEE Trans. Power Electron. 30, 547–560. https://doi.org/10.1109/TPEL.2014.2308251.

Faraji, F., Mousavi, G.S.M., Hajirayat, A., Birjandi, A.A.M., Al-Haddad, K., 2017. Single-stage single-phase three-level neutral-point-clamped transformerless grid-connected photovoltaic inverters: topology review. Renew. Sustain. Energy Rev. 80, 197–214. https://doi.org/10.1016/j.rser.2017.05.181.

Fathy, A., 2015. Reliable and efficient approach for mitigating the shading effect on photovoltaic module based on Modified Artificial Bee Colony algorithm. Renew. Energy 81, 78–88. https://doi.org/10.1016/j.renene.2015.03.017.

Feng, X., Wang, F., Wu, C., Luo, J., Zhang, L., 2019. Modeling and comparisons of aggregated flyback microinverters in aspect of harmonic resonances with the grid. IEEE Trans. Ind. Electron. 66, 276–285. https://doi.org/10.1109/TIE.2018.2821634.

Fermeiro, J.B.L., Pombo, J.A.N., Calado, M.R.A., Mariano, S.J.P.S., 2017. A new controller for DC-DC converters based on particle swarm optimization. Appl. Soft Comput. 52, 418–434. https://doi.org/10.1016/j.asoc.2016.10.025.

Furtado, A.M.S., Bradaschia, F., Cavalcanti, M.C., Limongi, L.R., 2018. A reduced voltage range global maximum power point tracking algorithm for photovoltaic systems under partial shading conditions. IEEE Trans. Ind. Electron. 65, 3252–3262. https://doi.org/10.1109/TIE.2017.2750623.

Gao, M., Chen, M., Zhang, C., Qian, Z., 2014. Analysis and implementation of an improved flyback inverter for photovoltaic AC module applications. IEEE Trans. Power Electron. 29, 3428–3444. https://doi.org/10.1109/TPEL.2013.2279266.

Godoy, R.B., Bizarro, D.B., de Andrade, E.T., de Oliveira Soares, J., Ribeiro, P.E.M.J., Carniato, L.A., Kimpara, M.L.M., Pinto, J.O.P., Al-Haddad, K., Canesin, C.A., 2017. Procedure to match the dynamic response of MPPT and droop-controlled microinverters. IEEE Trans. Ind. Appl. 53, 2358–2368. https://doi.org/10.1109/TIA.2016.2642883.

Goroohi Sardou, I., Zare, M., Azad-Farsani, E., 2018. Robust energy management of a microgrid with photovoltaic inverters in VAR compensation mode. Int. J. Electr. Power Energy Syst. 98, 118–132. https://doi.org/10.1016/j.ijepes.2017.11.037.

Gotekar, P.S., Muley, S.P., Kothari, D.P., Umre, B.S., 2015. Comparison of full bridge bipolar, H5, H6 and HERIC inverter for single phase photovoltaic systems - a review. In: 2015 Annual IEEE India Conference (INDICON). Presented at the 2015 Annual IEEE India Conference (INDICON). IEEE, New Delhi, India, pp. 1–6. https://doi.org/10.1109/INDICON.2015.7443837.

Guo, X., Jia, X., Lu, Z., Guerrero, J.M., 2016. Single phase cascaded H5 inverter with leakage current elimination for transformerless photovoltaic system. In: 2016 IEEE Applied Power Electronics Conference and Exposition (APEC). Presented at the 2016 IEEE Applied Power Electronics Conference and Exposition (APEC). IEEE, Long Beach, CA, USA, pp. 398–401. https://doi.org/10.1109/APEC.2016.7467903.

Shen, Guoqiao, Zhu, Xuancai, Zhang, Jun, Dehong, Xu., 2010. A New feedback method for PR current control of LCL-filter-based grid-connected inverter. IEEE Trans. Ind. Electron. 57, 2033–2041. https://doi.org/10.1109/TIE.2010.2040552.

Hadji, S., Gaubert, J.-P., Krim, F., 2015. Theoretical and experimental analysis of genetic algorithms based MPPT for PV systems. Energy Proc. 74, 772–787. https://doi.org/10.1016/j.egypro.2015.07.813.

Harrag, A., Messalti, S., 2019. IC-based variable step size neuro-fuzzy MPPT improving PV system performances. Energy Proc. 157, 362–374. https://doi.org/10.1016/j.egypro.2018.11.201.

Harrag, A., Messalti, S., 2015. Variable step size modified P&O MPPT algorithm using GA-based hybrid offline/online PID controller. Renew. Sustain. Energy Rev. 49, 1247–1260. https://doi.org/10.1016/j.rser.2015.05.003.

Hasan, R., Mekhilef, S., 2017. Highly efficient flyback microinverter for grid-connected rooftop PV system. Sol. Energy 146, 511–522. https://doi.org/10.1016/j.solener.2017.03.015.

Hasan, R., Mekhilef, S., Seyedmahmoudian, M., Horan, B., 2017. Grid-connected isolated PV microinverters: a review. Renew. Sustain. Energy Rev. 67, 1065–1080. https://doi.org/10.1016/j.rser.2016.09.082.

Hassaine, L., Olías, E., Quintero, J., Barrado, A., 2014. Power control for grid connected applications based on the phase shifting of the inverter output voltage with respect to the grid voltage. Int. J. Electr. Power Energy Syst. 57, 250–260. https://doi.org/10.1016/j.ijepes.2013.12.009.

Ho, C.N.-M., Cheung, V.S.P., Chung, H.S.-H., 2009. Constant-frequency hysteresis current control of grid-connected VSI without bandwidth control. IEEE Trans. Power Electron. 24, 2484–2495. https://doi.org/10.1109/TPEL.2009.2031804.

Hu, H., Harb, S., Fang, X., Zhang, D., Zhang, Q., Shen, Z.J., Batarseh, I., 2012. A three-port flyback for PV microinverter applications with power pulsation decoupling capability. IEEE Trans. Power Electron. 27, 3953–3964. https://doi.org/10.1109/TPEL.2012.2188840.

Hu, H., Harb, S., Kutkut, N.H., Shen, Z.J., Batarseh, I., 2013. A Single-stage microinverter

without using eletrolytic capacitors. IEEE Trans. Power Electron. 28, 2677–2687. https://doi.org/10.1109/TPEL.2012.2224886.
IEEE Standard 1547.2-2008, DeBlasio, R., 2009. IEEE Application Guide for IEEE Std 1547, IEEE Standard for Interconnecting Distributed Resources with Electric Power Systems, pp. 1–207.
International Electrotechnical Commission, Oruganti, R., 2014. IEC 61727-2004 Photovoltaic (PV) systems – Characteristics of the utility interface.
Islam, M., Mekhilef, S., 2014. An improved transformerless grid connected photovoltaic inverter with reduced leakage current. Energy Conv. Manage. 88, 854–862. https://doi.org/10.1016/j.enconman.2014.09.014.
Islam, M., Mekhilef, S., Hasan, M., 2015. Single phase transformerless inverter topologies for grid-tied photovoltaic system: a review. Renew. Sustain. Energy Rev. 45, 69–86. https://doi.org/10.1016/j.rser.2015.01.009.
Jaeger-Waldau, A., 2017. PV Status Report 2017 (Science for Policy). Joint Research Centre (JRC), Luxembourg.
Jana, J., Saha, H., Das Bhattacharya, K., 2017. A review of inverter topologies for single-phase grid-connected photovoltaic systems. Renew. Sustain. Energy Rev. 72, 1256–1270. https://doi.org/10.1016/j.rser.2016.10.049.
Jeong, Y., Kim, J.-K., Lee, J.-B., Moon, G.-W., 2017. An asymmetric half-bridge resonant converter having a reduced conduction loss for DC/DC power applications with a wide range of low input voltage. IEEE Trans. Power Electron. 32, 7795–7804. https://doi.org/10.1109/TPEL.2016.2639069.
Jiang, J.-A., Su, Y.-L., Kuo, K.-C., Wang, C.-H., Liao, M.-S., Wang, J.-C., Huang, C.-K., Chou, C.-Y., Lee, C.-H., Shieh, J.-C., 2017. On a hybrid MPPT control scheme to improve energy harvesting performance of traditional two-stage inverters used in photovoltaic systems. Renew. Sustain. Energy Rev. 69, 1113–1128. https://doi.org/10.1016/j.rser.2016.09.112.
Jiang, S., Cao, D., Li, Y., Peng, F.Z., 2012. Grid-connected boost-half-bridge photovoltaic microinverter system using repetitive current control and maximum power point tracking. IEEE Trans. Power Electron. 27, 4711–4722. https://doi.org/10.1109/TPEL.2012.2183389.
Joshi, P., Arora, S., 2017. Maximum power point tracking methodologies for solar PV systems – a review. Renew. Sustain. Energy Rev. 70, 1154–1177. https://doi.org/10.1016/j.rser.2016.12.019.
Jovanovic, M.M., Irving, B.T., 2016. On-the-fly topology-morphing control—efficiency optimization method for *LLC* resonant converters operating in wide input- and/or output-voltage range. IEEE Trans. Power Electron. 31, 2596–2608. https://doi.org/10.1109/TPEL.2015.2440099.
Jovanovic, M.M., Irving, B.T., 2015. Efficiency optimization of LLC resonant converters operating in wide input- and/or output-voltage range by on-the-fly topology-morphing control. In: 2015 IEEE Applied Power Electronics Conference and Exposition (APEC). Presented at the 2015 IEEE Applied Power Electronics Conference and Exposition (APEC). IEEE, Charlotte, NC, USA, pp. 1420–1427. https://doi.org/10.1109/APEC.2015.7104534.
Kabalci, E., 2018. The design and analysis of a two-stage PV converter with quasi-Z source inverter. In: 2018 IEEE 18th International Power Electronics and Motion Control Conference (PEMC). Presented at the 2018 IEEE 18th International Power Electronics and Motion Control Conference (PEMC). IEEE, Budapest, pp. 451–456. https://doi.org/10.1109/EPEPEMC.2018.8521953.
Kabalci, E., 2017. Maximum power point tracking (MPPT) algorithms for photovoltaic systems. In: Bizon, N., Mahdavi Tabatabaei, N., Blaabjerg, F., Kurt, E. (Eds.), Energy Harvesting and Energy Efficiency. Springer International Publishing, Cham, pp. 205–234. https://doi.org/10.1007/978-3-319-49875-1_8.
Kabalci, E., 2015. A smart monitoring infrastructure design for distributed renewable energy systems. Energy Convers. Manage. 90, 336–346. https://doi.org/10.1016/j.enconman.2014.10.062.
Kabalci, Ersan, Bayindir, R., Gokkus, G., Kabalci, Y., 2015a. Dual DC-DC converter and monitoring interface for asymmetrical string inverters. In: 2015 International Conference on Renewable Energy Research and Applications (ICRERA). IEEE, pp. 1580–1585.
Kabalci, E., Kabalci, Y., 2018. A wireless metering and monitoring system for solar string inverters. Electr. Power Energy Syst. 96, 282–295. https://doi.org/10.1016/j.ijepes.2017.10.013.
Kabalci, E., Kabalci, Y., Canbaz, R., Gokkus, G., 2015b. Single phase multilevel string inverter for solar applications. In: Presented at the 4th International Conference on Renewable Energy Research and Applications, Palermo Italy, pp. 109–114.
Kabalci, E., Kabalci, Y., Gokkus, G., 2015c. Dual DC-DC converter design for string inverters used in solar plants. In: Presented at the 4th International Conference on Renewable Energy Research and Applications, Palermo Italy, pp. 115–119.
Kabalci, Y., Kabalci, E., 2017. Modeling and analysis of a smart grid monitoring system for renewable energy sources. Sol. Energy 153, 262–275. https://doi.org/10.1016/j.solener.2017.05.063.
Karami, N., Moubayed, N., Outbib, R., 2017. General review and classification of different MPPT Techniques. Renew. Sustain. Energy Rev. 68, 1–18. https://doi.org/10.1016/j.rser.2016.09.132.
Kasa, N., Iida, T., Chen, L., 2005. Flyback inverter controlled by sensorless current MPPT for photovoltaic power system. IEEE Trans. Ind. Electron. 52, 1145–1152. https://doi.org/10.1109/TIE.2005.851602.
Kassem, A.M., 2012. MPPT control design and performance improvements of a PV generator powered DC motor-pump system based on artificial neural networks. Int. J. Electr. Power Energy Syst. 43, 90–98. https://doi.org/10.1016/j.ijepes.2012.04.047.
Kerekes, T., 2009. Analysis and Modeling of Transformerless Photovoltaic Inverter Systems. Aalborg University, Institute of Energy Technology, Aalborg.
Kerekes, T., Teodorescu, R., Rodriguez, P., Vazquez, G., Aldabas, E., 2011. A new high-efficiency single-phase transformerless PV inverter topology. IEEE Trans. Ind. Electron. 58, 184–191. https://doi.org/10.1109/TIE.2009.2024092.
Khan, A., Ben-Brahim, L., Gastli, A., Benammar, M., 2017. Review and simulation of leakage current in transformerless microinverters for PV applications. Renew. Sustain. Energy Rev. 74, 1240–1256. https://doi.org/10.1016/j.rser.2017.02.053.
Kim, Y.-H., Ji, Y.-H., Kim, J.-G., Jung, Y.-C., Won, C.-Y., 2013. A New control strategy for improving weighted efficiency in photovoltaic AC module-type interleaved flyback inverters. IEEE Trans. Power Electron. 28, 2688–2699. https://doi.org/10.1109/TPEL.2012.2226753.
Komurcugil, H., 2012. Rotating-sliding-line-based sliding-mode control for single-phase UPS inverters. IEEE Trans. Ind. Electron. 59, 3719–3726. https://doi.org/10.1109/TIE.2011.2159354.
Kouro, S., Leon, J.I., Vinnikov, D., Franquelo, L.G., 2015. Grid-connected photovoltaic systems: an overview of recent research and emerging PV converter technology. IEEE Ind. Electron. Mag. 9, 47–61. https://doi.org/10.1109/MIE.2014.2376976.
Kulaksız, A.A., Akkaya, R., 2012. A genetic algorithm optimized ANN-based MPPT algorithm for a stand-alone PV system with induction motor drive. Sol. Energy 86, 2366–2375. https://doi.org/10.1016/j.solener.2012.05.006.
Lai, C.M., 2014. A single-stage grid-connected PV micro-inverter based on interleaved flyback converter topology. In: 2014 International Symposium on Computer, Consumer and Control. Presented at the 2014 International Symposium on Computer, Consumer and Control (IS3C). IEEE, Taichung, Taiwan, pp. 187–190. https://doi.org/10.1109/IS3C.2014.59.
Lasheen, M., Rahman, A.K.A., Abdel-Salam, M., Ookawara, S., 2016. Performance enhancement of constant voltage based MPPT for photovoltaic applications using genetic algorithm. Energy Proc. 100, 217–222. https://doi.org/10.1016/j.egypro.2016.10.168.
Li, X., Wen, H., Hu, Y., Jiang, L., Xiao, W., 2018. Modified beta algorithm for GMPPT and partial shading detection in photovoltaic systems. IEEE Trans. Power Electron. 33, 2172–2186. https://doi.org/10.1109/TPEL.2017.2697459.
Zhang, Li, Sun, Kai, Yan Xing, Mu., Xing, 2014a. H6 Transformerless full-bridge PV grid-tied inverters. IEEE Trans. Power Electron. 29, 1229–1238. https://doi.org/10.1109/TPEL.2013.2260178.
Liu, Z., Wu, H., Liu, Y., Ji, J., Wu, W., Blaabjerg, F., 2017. Modelling of the modified-LLCL-filter-based single-phase grid-tied Aalborg inverter. IET Power Electron. 10, 151–155. https://doi.org/10.1049/iet-pel.2016.0044.
Lodh, T., Pragallapati, N., Agarwal, V., 2016. An improved control scheme for interleaved flyback converter based micro-inverter to achieve high efficiency. In: 2016 IEEE 1st International Conference on Power Electronics, Intelligent Control and Energy Systems (ICPEICES). Presented at the 2016 IEEE 1st International Conference on Power Electronics, Intelligent Control and Energy Systems (ICPEICES). IEEE, Delhi, India, pp. 1–6. https://doi.org/10.1109/ICPEICES.2016.7853693.
Mahela, O.P., Shaik, A.G., 2017. Comprehensive overview of grid interfaced solar photovoltaic systems. Renew. Sustain. Energy Rev. 68, 316–332. https://doi.org/10.1016/j.rser.2016.09.096.
Xingkui, Mao, Qisheng, Huang, Qingbo, Ke, Yudi, Xiao, Zhe, Zhang, Andersen, M.A.E., 2016. Grid-connected photovoltaic micro-inverter with new hybrid control LLC resonant converter. In: IECON 2016 - 42nd Annual Conference of the IEEE Industrial Electronics Society. Presented at the IECON 2016 - 42nd Annual Conference of the IEEE Industrial Electronics Society. IEEE, Florence, Italy, pp. 2319–2324. https://doi.org/10.1109/IECON.2016.7793632.
Masson, G., Kaizuka, I., Cambiè, C., 2018. Snapshot of Global Photovoltaıc Markets (PVPS No. Report IEA PVPS T1-33:2018). IEA International Energy Agency.
Mattavelli, P., 2005. An improved deadbeat control for UPS using disturbance observers. IEEE Trans. Ind. Electron. 52, 206–212. https://doi.org/10.1109/TIE.2004.837912.
Mekki, H., Mellit, A., Salhi, H., 2016. Artificial neural network-based modelling and fault detection of partial shaded photovoltaic modules. Simul. Model. Pract. Theory 67, 1–13. https://doi.org/10.1016/j.simpat.2016.05.005.
Meneses, D., Blaabjerg, F., García, Ó., Cobos, J.A., 2013. Review and comparison of step-up transformerless topologies for photovoltaic AC-module application. IEEE Trans. Power Electron. 28, 2649–2663. https://doi.org/10.1109/TPEL.2012.2227820.
Meneses, D., Garcia, O., Alou, P., Oliver, J.A., Cobos, J.A., 2015. Grid-connected forward microinverter with primary-parallel secondary-series transformer. IEEE Trans. Power Electron. 30, 4819–4830. https://doi.org/10.1109/TPEL.2014.2365760.
Messalti, S., Harrag, A., Loukriz, A., 2017. A new variable step size neural networks MPPT controller: review, simulation and hardware implementation. Renew. Sustain. Energy Rev. 68, 221–233. https://doi.org/10.1016/j.rser.2016.09.131.
Miret, J., Castilla, M., Matas, J., Guerrero, J.M., Vasquez, J.C., 2009. Selective harmonic-compensation control for single-phase active power filter with high harmonic rejection. IEEE Trans. Ind. Electron. 56, 3117–3127. https://doi.org/10.1109/TIE.2009.2024662.
Mirza, A.F., Ling, Q., Javed, M.Y., Mansoor, M., 2019. Novel MPPT techniques for photovoltaic systems under uniform irradiance and partial shading. Sol. Energy 184, 628–648. https://doi.org/10.1016/j.solener.2019.04.034.
Mohapatra, A., Nayak, B., Das, P., Mohanty, K.B., 2017. A review on MPPT techniques of PV system under partial shading condition. Renew. Sustain. Energy Rev. 80, 854–867. https://doi.org/10.1016/j.rser.2017.05.083.
Montoya, D.G., Ramos-Paja, C.A., Giral, R., 2016. Improved design of sliding-mode controllers based on the requirements of MPPT techniques. IEEE Trans. Power Electron. 31, 235–247. https://doi.org/10.1109/TPEL.2015.2397831.
Moon, S., Yoon, S.-G., Park, J.-H., 2015. A new low-cost centralized MPPT controller system for multiply distributed photovoltaic power conditioning modules. IEEE Trans. Smart Grid 6, 2649–2658. https://doi.org/10.1109/TSG.2015.2439037.
Mosaad, M.I., Abed El raouf, M.O., Al-Ahmar, M.A., Banakher, F.A., 2019. Maximum power point tracking of PV system based cuckoo search algorithm; review and comparison. Energy Procedia 162, 117–126. https://doi.org/10.1016/j.egypro.2019.04.013.
Muhsen, D.H., Nabil, M., Haider, H.T., Khatib, T., 2019. A novel method for sizing of

standalone photovoltaic system using multi-objective differential evolution algorithm and hybrid multi-criteria decision making methods. Energy 174, 1158–1175. https://doi.org/10.1016/j.energy.2019.03.046.
Nabipour, M., Razaz, M., Seifossadat, S.G., Mortazavi, S.S., 2017. A new MPPT scheme based on a novel fuzzy approach. Renew. Sustain. Energy Rev. 74, 1147–1169. https://doi.org/10.1016/j.rser.2017.02.054.
Oshaba, A.S., Ali, E.S., Abd Elazim, S.M., 2015. MPPT control design of PV system supplied SRM using BAT search algorithm. Sustain. Energy Grids Netw. 2, 51–60. https://doi.org/10.1016/j.segan.2015.04.002.
Öztürk, S., Poşpoş, P., Utalay, V., Koç, A., Ermiş, M., Çadırcı, I., 2018. Operating principles and practical design aspects of all SiC DC/AC/DC converter for MPPT in grid-connected PV supplies. Sol. Energy 176, 380–394. https://doi.org/10.1016/j.solener.2018.10.049.
Petreuş, D., Daraban, S., Ciocan, I., Patarau, T., Morel, C., Machmoum, M., 2013. Low cost single stage micro-inverter with MPPT for grid connected applications. Sol. Energy 92, 241–255. https://doi.org/10.1016/j.solener.2013.03.016.
Pilakkat, D., Kanthalakshmi, S., 2019. An improved P&O algorithm integrated with artificial bee colony for photovoltaic systems under partial shading conditions. Sol. Energy 178, 37–47. https://doi.org/10.1016/j.solener.2018.12.008.
Guo, Qian, Wang, Jun, Ma, Hao, 2014. Frequency adaptive repetitive controller for grid-connected inverter with an all-pass infinite impulse response (IIR) filter. In: 2014 IEEE 23rd International Symposium on Industrial Electronics (ISIE). Presented at the 2014 IEEE 23rd International Symposium on Industrial Electronics (ISIE). IEEE, Istanbul, Turkey, pp. 491–496. https://doi.org/10.1109/ISIE.2014.6864662.
Rajgor, G., 2013. Microinverters – a solar game changer. Renew. Energy Focus 14, 16–17. https://doi.org/10.1016/S1755-0084(13)70047-4.
Ramli, M.A.M., Ishaque, K., Jawaid, F., Al-Turki, Y.A., Salam, Z., 2015. A modified differential evolution based maximum power point tracker for photovoltaic system under partial shading condition. Energy Build. 103, 175–184. https://doi.org/10.1016/j.enbuild.2015.06.058.
Rezaei, M.A., Lee, K.-J., Huang, A.Q., 2016. A high-efficiency flyback micro-inverter with a new adaptive snubber for photovoltaic applications. IEEE Trans. Power Electron. 31, 318–327. https://doi.org/10.1109/TPEL.2015.2407405.
Rezk, H., Fathy, A., Abdelaziz, A.Y., 2017. A comparison of different global MPPT techniques based on meta-heuristic algorithms for photovoltaic system subjected to partial shading conditions. Renew. Sustain. Energy Rev. 74, 377–386. https://doi.org/10.1016/j.rser.2017.02.051.
Rezk, H., Hasaneen, E.-S., 2015. A new MATLAB/Simulink model of triple-junction solar cell and MPPT based on artificial neural networks for photovoltaic energy systems. Ain Shams Eng. J. 6, 873–881. https://doi.org/10.1016/j.asej.2015.03.001.
Rizzo, S.A., Scelba, G., 2015. ANN based MPPT method for rapidly variable shading conditions. Appl. Energy 145, 124–132. https://doi.org/10.1016/j.apenergy.2015.01.077.
Rizzoli, G., Mengoni, M., Zarri, L., Tani, A., Serra, G., Casadei, D., 2016. Comparison of single-phase H4, H5, H6 inverters for transformerless photovoltaic applications. In: IECON 2016 - 42nd Annual Conference of the IEEE Industrial Electronics Society. Presented at the IECON 2016 - 42nd Annual Conference of the IEEE Industrial Electronics Society. IEEE, Florence, Italy, pp. 3038–3045. https://doi.org/10.1109/IECON.2016.7792984.
Rojas, C.A., Aguirre, M., Kouro, S., Geyer, T., Gutierrez, E., 2017. Leakage current mitigation in photovoltaic string inverter using predictive control with fixed average switching frequency. IEEE Trans. Ind. Electron. 64, 9344–9354. https://doi.org/10.1109/TIE.2017.2708003.
Romero-Cadaval, E., Spagnuolo, G., Franquelo, L.G., Ramos-Paja, C.A., Suntio, T., Xiao, W.M., 2013. Grid-connected photovoltaic generation plants: components and operation. IEEE Ind. Electron. Mag. 7, 6–20. https://doi.org/10.1109/MIE.2013.2264540.
Saad, N.H., El-Sattar, A.A., Mansour, A.E.-A.M., 2018. A novel control strategy for grid connected hybrid renewable energy systems using improved particle swarm optimization. Ain Shams Eng. J. 9, 2195–2214. https://doi.org/10.1016/j.asej.2017.03.009.
Salam, Z., Ahmed, J., Merugu, B.S., 2013. The application of soft computing methods for MPPT of PV system: a technological and status review. Appl. Energy 107, 135–148. https://doi.org/10.1016/j.apenergy.2013.02.008.
Saravanan, S., Ramesh Babu, N., 2016. RBFN based MPPT algorithm for PV system with high step up converter. Energy Conv. Manage. 122, 239–251. https://doi.org/10.1016/j.enconman.2016.05.076.
Sasidharan, N., Singh, J.G., 2017. A novel single-stage single-phase reconfigurable inverter topology for a solar powered hybrid AC/DC home. IEEE Trans. Ind. Electron. 64, 2820–2828. https://doi.org/10.1109/TIE.2016.2643602.
Schmela, M., 2018. Global Market Outlook for Solar Power/2018–2022. SolarPower Europe, Brussels, Belgium.
Schweizer, M., Kolar, J.W., 2013. Design and implementation of a highly efficient three-level T-type converter for low-voltage applications. IEEE Trans. Power Electron. 28, 899–907. https://doi.org/10.1109/TPEL.2012.2203151.
Serban, E., Paz, F., Ordonez, M., 2017. Improved PV inverter operating range using a miniboost. IEEE Trans. Power Electron. 32, 8470–8485. https://doi.org/10.1109/TPEL.2016.2641478.
Shams El-Dein, M.Z., Kazerani, M., Salama, M.M.A., 2013a. An optimal total cross tied interconnection for reducing mismatch losses in photovoltaic arrays. IEEE Trans. Sustainable Energy 4, 99–107. https://doi.org/10.1109/TSTE.2012.2202325.
Shams El-Dein, M.Z., Kazerani, M., Salama, M.M.A., 2013b. Optimal photovoltaic array reconfiguration to reduce partial shading losses. IEEE Trans. Sustain. Energy 4, 145–153. https://doi.org/10.1109/TSTE.2012.2208128.
Shayestegan, M., Shakeri, M., Abunima, H., Reza, S.M.S., Akhtaruzzaman, M., Bais, B., Mat, S., Sopian, K., Amin, N., 2018. An overview on prospects of new generation single-phase transformerless inverters for grid-connected photovoltaic (PV) systems. Renew. Sustain. Energy Rev. 82, 515–530. https://doi.org/10.1016/j.rser.2017.09.055.
Sher, H.A., Addoweesh, K.E., 2012. Micro-inverters — promising solutions in solar photovoltaics. Energy Sustain. Devel. 16, 389–400. https://doi.org/10.1016/j.esd.2012.10.002.
Shimizu, T., Wada, K., Nakamura, N., 2006. Flyback-type single-phase utility interactive inverter with power pulsation decoupling on the DC input for an AC photovoltaic module system. IEEE Trans. Power Electron. 21, 1264–1272. https://doi.org/10.1109/TPEL.2006.880247.
Siwakoti, Y.P., Blaabjerg, F., 2018. Common-ground-type transformerless inverters for single-phase solar photovoltaic systems. IEEE Trans. Ind. Electron. 65, 2100–2111. https://doi.org/10.1109/TIE.2017.2740821.
Sridhar, V., Umashankar, S., 2017. A comprehensive review on CHB MLI based PV inverter and feasibility study of CHB MLI based PV-STATCOM. Renew. Sustain. Energy Rev. 78, 138–156. https://doi.org/10.1016/j.rser.2017.04.111.
Sukesh, N., Pahlevaninezhad, M., Jain, P.K., 2014. Analysis and implementation of a single-stage flyback PV microinverter with soft switching. IEEE Trans. Ind. Electron. 61, 1819–1833. https://doi.org/10.1109/TIE.2013.2263778.
Sun, X., Li, X., Shen, Y., Wang, B., Guo, X., 2017. Dual-bridge LLC resonant converter with fixed-frequency PWM control for wide input applications. IEEE Trans. Power Electron. 32, 69–80. https://doi.org/10.1109/TPEL.2016.2530748.
Sundareswaran, K., Vignesh Kumar, V., Palani, S., 2015. Application of a combined particle swarm optimization and perturb and observe method for MPPT in PV systems under partial shading conditions. Renew. Energy 75, 308–317. https://doi.org/10.1016/j.renene.2014.09.044.
Tajuddin, M.F.N., Ayob, S.M., Salam, Z., Saad, M.S., 2013. Evolutionary based maximum power point tracking technique using differential evolution algorithm. Energy Build. 67, 245–252. https://doi.org/10.1016/j.enbuild.2013.07.085.
Tayebi, S.M., Hu, H., Batarseh, I., 2019. Advanced DC-link voltage regulation and capacitor optimization for three-phase microinverters. IEEE Trans. Ind. Electron. 66, 307–317. https://doi.org/10.1109/TIE.2018.2823700.
Thang, T.V., Thao, N.M., Jang, J.-H., Park, J.-H., 2014. Analysis and design of grid-connected photovoltaic systems with multiple-integrated converters and a pseudo-DC-link inverter. IEEE Trans. Ind. Electron. 61, 3377–3386. https://doi.org/10.1109/TIE.2013.2281153.
Titri, S., Larbes, C., Toumi, K.Y., Benatchba, K., 2017. A new MPPT controller based on the Ant colony optimization algorithm for Photovoltaic systems under partial shading conditions. Appl. Soft Comput. 58, 465–479. https://doi.org/10.1016/j.asoc.2017.05.017.
Tofigh Azary, M., Sabahi, M., Babaei, E., Abbasi Aghdam, Meinagh, F., 2018. Modified single-phase single-stage grid-tied flying inductor inverter with MPPT and suppressed leakage current. IEEE Trans. Ind. Electron. 65, 221–231. https://doi.org/10.1109/TIE.2017.2719610.
Vazquez, N., Rosas, M., Hernandez, C., Vazquez, E., Perez-Pinal, F.J., 2015. A new common-mode transformerless photovoltaic inverter. IEEE Trans. Ind. Electron. 62, 6381–6391. https://doi.org/10.1109/TIE.2015.2426146.
Vinnikov, D., Chub, A., Liivik, E., Kosenko, R., Korkh, O., 2019. Solar optiverter—a novel hybrid approach to the photovoltaic module level power electronics. IEEE Trans. Ind. Electron. 66, 3869–3880. https://doi.org/10.1109/TIE.2018.2850036.
Vinnikov, D., Chub, A., Liivik, E., Roasto, I., 2017. High-performance quasi-Z-source series resonant DC–DC converter for photovoltaic module-level power electronics applications. IEEE Trans. Power Electr. 32, 3634–3650. https://doi.org/10.1109/TPEL.2016.2591726.
Wang, F., Feng, X., Zhang, L., Du, Y., Su, J., 2018a. Impedance-based analysis of grid harmonic interactions between aggregated flyback micro-inverters and the grid. IET Power Electron. 11, 453–459. https://doi.org/10.1049/iet-pel.2017.0356.
Wang, H., Wu, W., Chung, H.S., Blaabjerg, F., 2018b. Coupled-inductor-based Aalborg inverter with input DC energy regulation. IEEE Trans. Ind. Electron. 65, 3826–3836. https://doi.org/10.1109/TIE.2017.2760849.
Xia, Y., Roy, J., Ayyanar, R., 2017. A capacitance-minimized, doubly grounded transformer less photovoltaic inverter with inherent active-power decoupling. IEEE Trans. Power Electron. 32, 5188–5201. https://doi.org/10.1109/TPEL.2016.2606344.
Xiao, H., Xie, S., Chen, Y., Huang, R., 2011. An optimized transformerless photovoltaic grid-connected inverter. IEEE Trans. Ind. Electron. 58, 1887–1895. https://doi.org/10.1109/TIE.2010.2054056.
Xiao, H.F., Lan, K., Zhang, L., 2015. A quasi-unipolar SPWM full-bridge transformerless PV grid-connected inverter with constant common-mode voltage. IEEE Trans. Power Electron. 30, 3122–3132. https://doi.org/10.1109/TPEL.2014.2331367.
Xiao, H.F., Zhang, L., Li, Y., 2017. A zero-voltage-transition HERIC-type transformerless photovoltaic grid-connected inverter. IEEE Trans. Ind. Electron. 64, 1222–1232. https://doi.org/10.1109/TIE.2016.2611574.
Xiong, G., Zhang, J., Yuan, X., Shi, D., He, Y., Yao, G., 2018. Parameter extraction of solar photovoltaic models by means of a hybrid differential evolution with whale optimization algorithm. Sol. Energy 176, 742–761. https://doi.org/10.1016/j.solener.2018.10.050.
Xu, J., Xie, S., Tang, T., 2014. Active damping-based control for grid-connected LCL -filtered inverter with injected grid current feedback only. IEEE Trans. Ind. Electron. 61, 4746–4758. https://doi.org/10.1109/TIE.2013.2290771.
Yahya, A., El Fadil, H., Oulcaid, M., Ammeh, L., Giri, F., Guerrero, J.M., 2018. Control of grid connected photovoltaic systems with microinverters: new theoretical design and numerical evaluation: advanced control of microinverters. Asian J. Control 20, 906–918. https://doi.org/10.1002/asjc.1704.
Yang, B., Zhong, L., Zhang, X., Shu, H., Yu, T., Li, H., Jiang, L., Sun, L., 2019. Novel bio-inspired memetic salp swarm algorithm and application to MPPT for PV systems considering partial shading condition. J. Cleaner Prod. 215, 1203–1222. https://doi.

org/10.1016/j.jclepro.2019.01.150.
Yao, Z., Xiao, L., 2013. Control of single-phase grid-connected inverters with nonlinear loads. IEEE Trans. Ind. Electron. 60, 1384–1389. https://doi.org/10.1109/TIE.2011.2174535.
Yilmaz, U., Kircay, A., Borekci, S., 2018. PV system fuzzy logic MPPT method and PI control as a charge controller. Renew. Sustain. Energy Rev. 81, 994–1001. https://doi.org/10.1016/j.rser.2017.08.048.
Zaki Diab, A.A., Rezk, H., 2017. Global MPPT based on flower pollination and differential evolution algorithms to mitigate partial shading in building integrated PV system. Sol. Energy 157, 171–186. https://doi.org/10.1016/j.solener.2017.08.024.
Zapata, J.W., Renaudineau, H., Kouro, S., Perez, M.A., Meynard, T.A., 2016. Partial power DC-DC converter for photovoltaic microinverters. In: IECON 2016 - 42nd Annual Conference of the IEEE Industrial Electronics Society. Presented at the IECON 2016 - 42nd Annual Conference of the IEEE Industrial Electronics Society. IEEE, Florence, Italy, pp. 6740–6745. https://doi.org/10.1109/IECON.2016.7793098.
Zeb, K., Uddin, W., Khan, M.A., Ali, Z., Ali, M.U., Christofides, N., Kim, H.J., 2018. A comprehensive review on inverter topologies and control strategies for grid connected photovoltaic system. Renew. Sustain. Energy Rev. 94, 1120–1141. https://doi.org/10.1016/j.rser.2018.06.053.
Zeddini, Mohamed, A., Pusca, R., Sakly, A., Mimouni, M.F., 2016. PSO-based MPPT control of wind-driven self-excited induction generator for pumping system. Renew. Energy 95, 162–177. https://doi.org/10.1016/j.renene.2016.04.008.
Zhang, Q., 2013. Optimization and Design of Photovoltaic Micro-Inverter. University of Central Florida, Florida USA.
Zhang, Z., Chen, M., Chen, W., Jiang, C., Qian, Z., 2014b. Analysis and implementation of phase synchronization control strategies for BCM interleaved flyback microinverters. IEEE Trans. Power Electron. 29, 5921–5932. https://doi.org/10.1109/TPEL.2014.2300483.
Zhang, Zhe, Chen, M., Chen, W., Qian, Z., 2013a. Design and Analysis of the synchronization control method for BCM/DCM current-mode flyback micro-inverter. In: 2013 Twenty-Eighth Annual IEEE Applied Power Electronics Conference and Exposition (APEC). Presented at the 2013 IEEE Applied Power Electronics Conference and Exposition - APEC 2013. IEEE, Long Beach, CA, USA, pp. 68–75. https://doi.org/10.1109/APEC.2013.6520187.
Zhang, Zhiliang, He, X.-F., Liu, Y.-F., 2013b. An optimal control method for photovoltaic grid-tied-interleaved flyback microinverters to achieve high efficiency in wide load range. IEEE Trans. Power Electron. 28, 5074–5087. https://doi.org/10.1109/TPEL.2013.2245919.
Zhang, Z., Zhang, J., Shao, S., 2018. A variable off-time control method for a single-phase DCM microinverter. IEEE Trans. Power Electron. 33, 7229–7239. https://doi.org/10.1109/TPEL.2017.2759227.
Zhang, Z., Zhang, Junming, Shao, S., Zhang, Junjun, 2019. A High-efficiency single-phase T-type BCM microinverter. IEEE Trans. Power Electron. 34, 984–995. https://doi.org/10.1109/TPEL.2018.2824342.
Zhao, F., Xue, F., Zhang, Y., Ma, W., Zhang, C., Song, H., 2018. A hybrid algorithm based on self-adaptive gravitational search algorithm and differential evolution. Expert Syst. Appl. 113, 515–530. https://doi.org/10.1016/j.eswa.2018.07.008.
Zhu, M., Zhao, Q., Ye, Y., Xu, G., 2016. Improved repetitive control scheme for grid-connected inverter with frequency adaptation. IET Power Electron. 9, 883–890. https://doi.org/10.1049/iet-pel.2015.0057.